Tumor Necrosis Factor-α–Mediated Downregulation of the Cystic Fibrosis Transmembrane Conductance Regulator Drives Pathological Sphingosine-1-Phosphate Signaling in a Mouse Model of Heart Failure

Anja Meissner, Jingli Yang, Jeffrey T. Kroetsch, Meghan Sauvé, Hendrik Dax, Abdul Momen, M. Hossein Noyan-Ashraf, Scott Heximer, Mansoor Husain, Darcy Lidington and Steffen-Sebastian Bolz

Circulation. 2012;125:2739-2750; originally published online April 25, 2012;
doi: 10.1161/CIRCULATIONAHA.111.047316
Circulation is published by the American Heart Association, 7272 Greenville Avenue, Dallas, TX 75231

Print ISSN: 0009-7322. Online ISSN: 1524-4539

Tumor Necrosis Factor-α–Mediated Downregulation of the Cystic Fibrosis Transmembrane Conductance Regulator Drives Pathological Sphingosine-1-Phosphate Signaling in a Mouse Model of Heart Failure

Anja Meissner, PhD; Jingli Yang, MD; Jeffrey T. Kroetsch, MSc; Meghan Sauvé, MSc; Hendrik Dax, MD; Abdul Momen, MD; M. Hossein Noyan-Ashraf, PhD; Scott Heximer, PhD; Mansoor Husain, MD; Darcy Lidington, PhD; Steffen-Sebastian Bolz, MD, PhD

Background—Sphingosine-1-phosphate (S1P) signaling is a central regulator of resistance artery tone. Therefore, S1P levels need to be tightly controlled through the delicate interplay of its generating enzyme sphingosine kinase 1 and its functional antagonist S1P phosphohydrolase-1. The intracellular localization of S1P phosphohydrolase-1 necessitates the import of extracellular S1P into the intracellular compartment before its degradation. The present investigation proposes that the cystic fibrosis transmembrane conductance regulator transports extracellular S1P and hence modulates microvascular S1P signaling in health and disease.

Methods and Results—In cultured murine vascular smooth muscle cells in vitro and isolated murine mesenteric and posterior cerebral resistance arteries ex vivo, the cystic fibrosis transmembrane conductance regulator (1) is critical for S1P uptake; (2) modulates S1P-dependent responses; and (3) is downregulated in vitro and in vivo by tumor necrosis factor-α, with significant functional consequences for S1P signaling and vascular tone. In heart failure, tumor necrosis factor-α downregulates the cystic fibrosis transmembrane conductance regulator across several organs, including the heart, lung, and brain, suggesting that it is a fundamental mechanism with implications for systemic S1P effects.

Conclusions—We identify the cystic fibrosis transmembrane conductance regulator as a critical regulatory site for S1P signaling; its tumor necrosis factor-α–dependent downregulation in heart failure underlies an enhancement in microvascular tone. This molecular mechanism potentially represents a novel and highly strategic therapeutic target for cardiovascular conditions involving inflammation. **(*Circulation*. 2012;125:2739-2750.)**

Key Words: acute myocardial infarction ■ hemodynamics ■ myogenic vasoconstriction ■ signal transduction ■ vasomotor tone

Sphingosine-1-phosphate (S1P) is a ubiquitous signaling mediator that directs a diverse array of biological processes.[1] In the microcirculation, S1P is a potent vasoconstrictor and a central mediator regulating myogenic tone.[2–5] This confers S1P signaling with significant importance in the control of blood flow autoregulation, tissue perfusion, and systemic blood pressure.

Editorial see p 2692
Clinical Perspective on p 2750

The potent and pleiotropic effects of S1P are confined both spatially and temporally[6]; however, the molecular mechanisms limiting S1P bioavailability are not completely understood. We have demonstrated that S1P phosphohydrolase-1 (SPP1), an intracellular enzyme primarily localized to the endoplasmic reticulum,[7,8] degrades extracellular S1P.[3] As a consequence, we concluded that an S1P "import" mechanism must be present in vascular smooth muscle cells. Boujaoude et al[9] have provided indirect evidence that the cystic fibrosis transmembrane conductance regulator (CFTR) could act as this S1P transporter and thereby limit S1P receptor–mediated effects. Accordingly, we have observed that CFTR inhibition specifically enhances responses known to rely on S1P in skeletal muscle resistance arteries.[3]

Received June 3, 2011; accepted March 20, 2012.

From the Department of Physiology (A.M., J.Y., J.T.K., M.S., H.D., M.H.N.-A., S.H., M.H., D.L., S.B.), Heart and Stroke/Richard Lewar Centre of Excellence for Cardiovascular Research (S.H., M.H., S.B.), and Department of Medicine (M.H.), University of Toronto; Division of Cell and Molecular Biology, Toronto General Hospital Research Institute (A.M., M.H.N.-A., M.H.); and Toronto Centre for Microvascular Medicine, University of Toronto, and Li Ka Shing Knowledge Institute at St Michael's Hospital (D.L., S.B.), Toronto, Ontario, Canada.

The online-only Data Supplement is available with this article at http://circ.ahajournals.org/lookup/suppl/doi:10.1161/CIRCULATIONAHA.111.047316/-/DC1.

Correspondence to Steffen-Sebastian Bolz, MD, PhD, Department of Physiology, Heart and Stroke/Richard Lewar Centre of Excellence in Cardiovascular Research, University of Toronto, Medical Science Building, Room 3326, 1 King's College Circle, Toronto, Ontario, M5S 1A8 Canada. E-mail sts.bolz@utoronto.ca

Circulation **is available at http://circ.ahajournals.org** **DOI: 10.1161/CIRCULATIONAHA.111.047316**

Proper CFTR function requires the orchestrated regulation of expression, localization, and gating. On the basis of our proposed model that CFTR transports extracellular S1P across the plasma membrane for degradation, the disruption of any of these aspects would be expected to affect S1P signaling. This leads us to speculate that CFTR dysfunction could play a causal role in pathological conditions that are associated with altered S1P signaling.[10–12] The prominent enhancement of S1P signaling in resistance arteries under the condition of heart failure (HF)[4,5] is a prime example advanced in the present investigation.

In the present study, we demonstrate that an inverse relationship between microvascular CFTR activity and S1P signaling is manifest both in well-defined S1P-dependent vasomotor responses and myogenic tone[2,13,14] and in mice with HF, a disease model in which S1P is known to mediate enhanced peripheral vascular resistance.[4]

Methods

This investigation conforms to the *Guide for the Care and Use of Laboratory Animals* published by the National Institutes of Health (publication No. 85-23, revised 1996). All animal care and experimental protocols were approved by the institutional animal care and use committees at the University of Toronto and the University Health Network, Toronto, and were conducted in accordance with Canadian animal protection laws.

Animals

Wild-type mice (aged 2–3 months; C57BL6) were purchased commercially from Charles River Laboratories (Montreal, Quebec, Canada). Tumor necrosis factor-α (TNF-α) knockout mice ($TNF\alpha^{-/-}$)[15] were purchased commercially from Taconic Laboratories (Hudson, NY). CFTR knockout mice ($CFTR^{-/-}$)[16] were obtained from an established colony maintained at the Hospital for Sick Children, Toronto. All mice were housed under a standard 12-hour/12-hour light/dark cycle, were fed normal chow, and had access to water ad libitum.

Preparation of Cultured Primary Mesenteric Artery Smooth Muscle Cells

Mesenteric artery segments were isolated, cut into small pieces, and digested with trypsin, collagenase, and elastase. The resulting cell suspension was washed several times in phosphate-buffered saline and plated in Dulbecco's modified Eagle's medium containing 10% fetal bovine serum and 1% penicillin-streptomycin. Cell cultures were maintained at 37°C with 5% CO_2 split at a seeding density of 10^6 cells. Immunostaining for α-actin, positive polymerase chain reaction results for myocardin and MyoD, and negative polymerase chain reaction results for endothelial NO synthase confirmed smooth muscle cell identity.

Fluorescence-Activated Cell Sorting–Based Measurement of Fluorescein Isothiocyanate–S1P Uptake

A fluorescence-activated cell sorting (FACS)–based approach to semiquantitatively measure the uptake of S1P–fluorescein isothiocyanate (FITC) has been published previously.[17] Briefly, cell monolayers (treated or untreated) were incubated with 1 μmol/L S1P-FITC for 60 minutes; the cells were then detached by trypsinization, washed twice with ice-cold phosphate-buffered saline, filtered through a 70-μm cell strainer, and analyzed with the use of the Becton-Dickinson FACS Canto operated by FACS DIVA version 6.1 software. Cell monolayers treated with unlabeled S1P served as background controls. The analysis procedure determined the median fluorescence intensity (arbitrary units) of each cell population, which is a measure of uptake.

Isolation and Functional Assessment of Cerebral Arteries

Experiments utilized both mouse posterior cerebral arteries (PCAs)[5] and mesenteric arteries.[4] After careful dissection, artery segments were cannulated on glass micropipettes, stretched to their in vivo lengths, and pressurized to 45 mm Hg. All functional experiments were conducted in 3-(*N*-morpholino)propanesulfonic acid (MOPS)–buffered saline at 37°C with no perfusion.

To measure myogenic responses, vessels were subjected to stepwise increases in transmural pressure (increments of 20 mm Hg) from 20 to 100 mm Hg. At each pressure step, vessel diameter (dia_{active}) was measured once a steady state was reached (3–5 minutes). Myogenic tone was calculated as the percent constriction in relation to the maximal diameter at each respective transmural pressure, as follows: tone (% of dia_{max})=[($dia_{max}-dia_{active}$)/dia_{max}]×100, where dia_{active} is the vessel diameter in MOPS containing Ca^{2+}, and dia_{max} is the diameter in Ca^{2+}-free MOPS.

Receptor-stimulated vasomotor responses were determined with the same calculation, but in this case, dia_{active} represents the vessel diameter at steady state after application of the given agent, and dia_{max} represents the maximal diameter (measured under Ca^{2+}-free conditions) at 45 mm Hg. Complete details are provided in the online-only Data Supplement.

Myocardial Infarction

HF in mice was induced by experimental myocardial infarction produced by surgical ligation of the left anterior descending (LAD) coronary artery.[4] Briefly, mice were anesthetized with isoflurane, intubated with a 20-gauge angiocatheter, and ventilated with room air. Under sterile conditions, the thorax and pericardium were opened, and the LAD was permanently ligated with 7-0 silk suture (Deknatel; Fall River). In sham-operated controls, the thorax and pericardium were opened, but the LAD was not ligated. After the procedure, the chest was closed, and the mice were extubated on spontaneous respiration. Cerebral arteries were isolated 4 to 6 weeks after myocardial infarction. As described,[4] HF mice develop enlarged hearts, congested lungs, and reduced cardiac output and blood pressure, with elevated peripheral resistance. All of these parameters remained normal in sham-operated controls.

Western Blots, Reverse Transcription Polymerase Chain Reaction, and Cell Proliferation Assessment

Standard biochemical procedures were utilized for experiments involving reverse transcription polymerase chain reaction and Western blots, including the fractionation of cellular lysates procedure in the latter case. A standard cell-counting approach was used to assess cell proliferation. Methodological details are provided in the online-only Data Supplement.

Statistical Analysis

All data are expressed as mean±SEM, where n is the number of independent experiments. A nonparametric Wilcoxon test with computation of exact *P* values was utilized for the comparison of 2 independent groups. For comparison of multiple independent groups, a nonparametric 1-way ANOVA (Kruskal-Wallis) followed by a Wilcoxon test with exact *P* value computation as a post hoc test for pairwise comparisons was used (because this was exploratory, we did not adjust for multiple comparisons). For the assessment of myogenic responses and dose-response relationships, data were analyzed with a 2-way repeated-measures ANOVA; if a significant effect of treatment/genotype was observed, the Wilcoxon test with exact *P* value computation was employed post hoc to assess the differences. Differences were considered significant at error probabilities of $P<0.05$. A Pearson correlation analysis was used for correlative assessments.

Results

CFTR Is Essential for S1P Import Into Vascular Smooth Muscle Cells

We first confirmed the expression of CFTR mRNA throughout the mouse vascular tree, including conduit and resistance

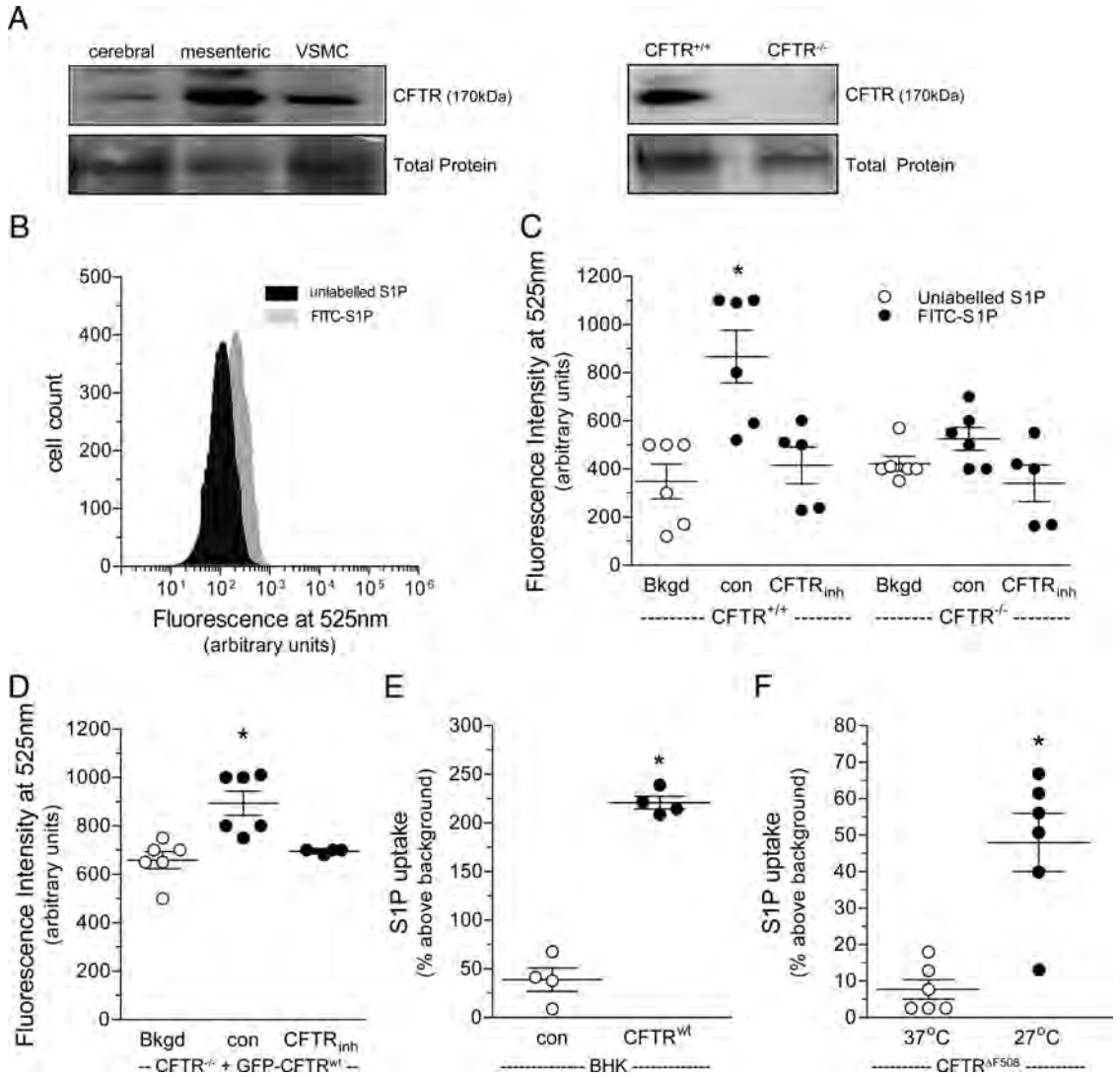

Figure 1. The cystic fibrosis transmembrane conductance regulator (CFTR) mediates cellular fluorescein isothiocyanate (FITC)–sphingosine-1-phosphate (S1P) uptake. **A**, Western blots confirm CFTR protein expression in isolated mouse cerebral and mesenteric arteries, as well as primary vascular smooth muscle cells (VSMCs) isolated from mouse mesenteric arteries. No CFTR signal was detected from mesenteric VSMCs isolated from CFTR knockout ($CFTR^{-/-}$) mice. The blots displayed are representative of at least 3 separate experiments. **B**, A standard fluorescence-activated cell sorting analysis technique reveals a shift in the median fluorescence intensity at 525 nm for VSMCs incubated with FITC-S1P compared with cells incubated with unlabeled S1P (background [Bkgd]). This median shift represents a measure of FITC-S1P uptake. **C**, In wild-type littermate VSMCs ($CFTR^{+/+}$), the median fluorescence intensity shift (n=6) is abolished by CFTR inhibition [100 nmol/L CFTR(inh)-172 for 30 minutes; n=5]. In VSMCs isolated from CFTR knockout mice, no shift in median fluorescence intensity is observed after FITC-S1P treatment (n=6), nor is there an effect of CFTR inhibition (n=5). Con indicates control. **D**, The S1P uptake deficit in $CFTR^{-/-}$ VSMCs was rescued by transfecting the cells with a wild-type CFTR construct ($CFTR^{wt}$; n=6); the rescued S1P uptake was abolished by CFTR inhibition (n=5). **E**, In baby hamster kidney (BHK) cells, stable expression of $CFTR^{wt}$ significantly increased S1P uptake compared with nontransfected cells (n=4). **F**, Maintaining BHK cells that express $CFTR^{\Delta F508}$ at 27°C for 24 hours (a procedure that increases plasma membrane abundance of CFTR) also significantly increased S1P uptake (n=6). *$P<0.05$ for multiple, unpaired comparisons within each genotype in **C**; multiple, unpaired comparisons in **D**; and single, unpaired comparisons in **E** and **F**. **E** and **F** display data normalized to their respective backgrounds.

arteries (Figure I in the online-only Data Supplement). Expression of CFTR protein was confirmed in mouse posterior cerebral and mesenteric arteries and in primary vascular smooth muscle cells (VSMCs) derived from mouse mesenteric arteries (Figure 1A).

Using a standard FACS assay and a pharmacological CFTR inhibitor [CFTR(inh)-172], we next demonstrated CFTR-dependent accumulation of FITC-labeled S1P (FITC-S1P) in VSMCs (Figure 1B and 1C). Control experiments demonstrated that coincubating unlabeled and FITC-labeled S1P significantly inhibited FITC-S1P uptake (Figure II in the online-only Data Supplement). FITC-S1P uptake was absent in VSMCs isolated from mice lacking CFTR ($CFTR^{-/-}$; Figure 1C), a deficiency rescued by expression of a green fluorescent protein (GFP)–tagged CFTR construct (GFP-$CFTR^{wt}$) and then abolished again by CFTR(inh)-172 (Figure 1D).

To more directly link S1P transport to CFTR expression and membrane localization, we studied immortalized baby hamster kidney cells, which possess a minimal endogenous level of CFTR. Baby hamster kidney cells exhibited a low

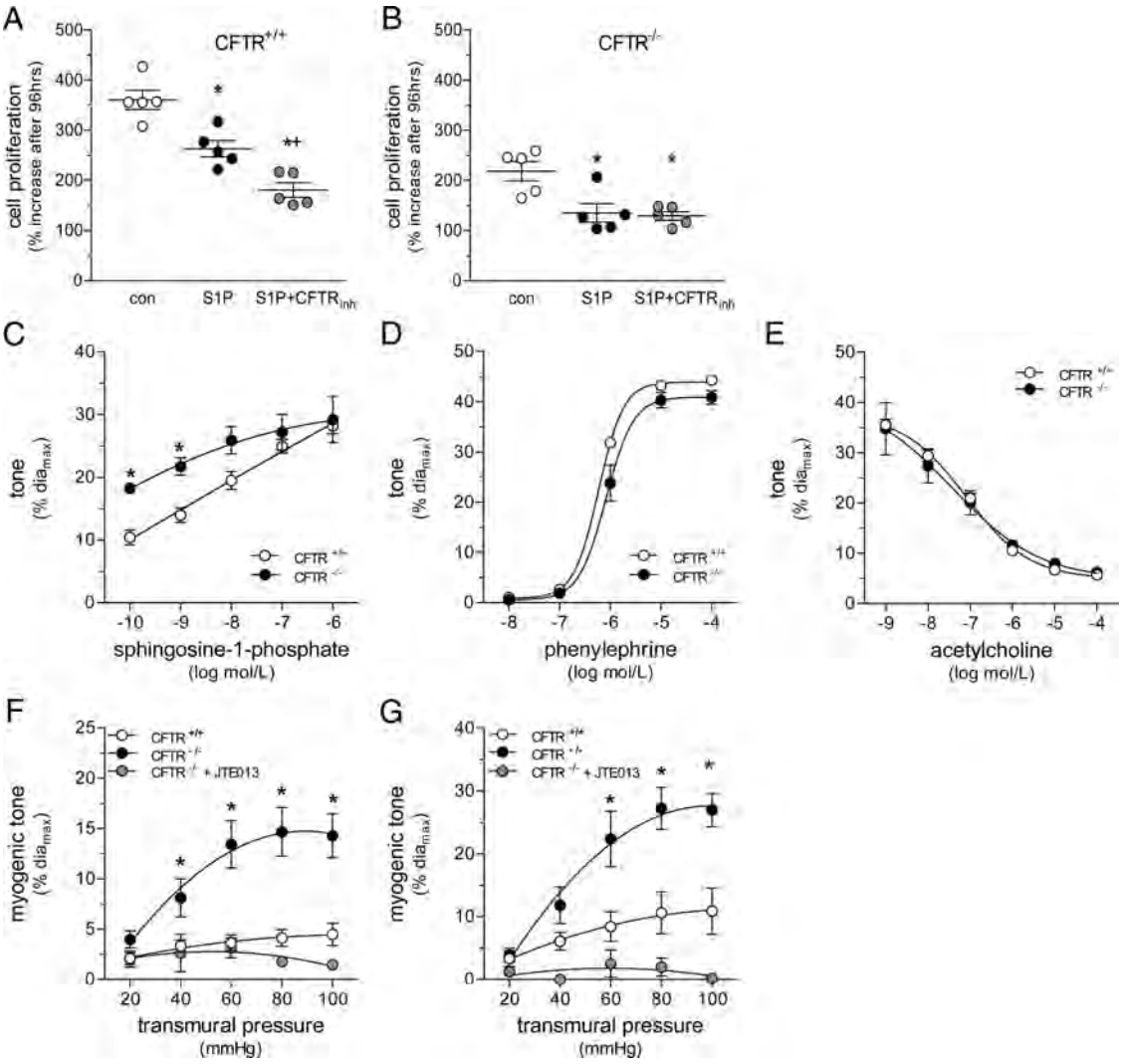

Figure 2. The cystic fibrosis transmembrane conductance regulator (CFTR) modulates sphingosine-1-phosphate (S1P)–dependent responses in cultured vascular smooth muscle cells and isolated arteries. **A**, S1P (100 nmol/L) significantly inhibits wild-type ($CFTR^{+/+}$) vascular smooth muscle cell proliferation, an effect that is enhanced by CFTR inhibition [100 nmol/L CFTR(inh)-172; n=5 for all groups]. **B**, CFTR knockout ($CFTR^{-/-}$) vascular smooth muscle cell proliferation is lower under control (con) conditions than $CFTR^{+/+}$ vascular smooth muscle cells ($P<0.05$ comparing white bars in **A** and **B**; n=5). S1P inhibits cell proliferation in $CFTR^{-/-}$ vascular smooth muscle cells; however, CFTR inhibition has no further effect (n=5). **C**, S1P-stimulated vasoconstriction is stronger in posterior cerebral arteries isolated from $CFTR^{-/-}$ compared with $CFTR^{+/+}$ littermate controls (n=6 for both groups). Posterior cerebral artery responses to phenylephrine (**D**) and acetylcholine (**E**) are similar in the 2 genotypes (n=4 for $CFTR^{+/+}$; n=3 for $CFTR^{-/-}$). **F**, Posterior cerebral artery myogenic tone is stronger at all transmural pressures >20 mm Hg (ie, 40–100 mm Hg); a similar pattern is observed for mesenteric arteries (**G**) (for both cerebral and mesenteric arteries: n=6 for $CFTR^{+/+}$; n=8 for $CFTR^{-/-}$). The enhanced myogenic tone in $CFTR^{-/-}$ cerebral (**F**) and mesenteric (**G**) arteries is abolished by $S1P_2$ receptor inhibition (1 μmol/L JTE013; 30 minutes; n=4 for both artery types). Maximal vessel diameters at 45 mm Hg (dia_{max}) were as follows: posterior cerebral artery $CFTR^{+/+}$ 166±8 μm (n=8), posterior cerebral artery $CFTR^{-/-}$ 162±5 μm (n=6), P=NS; and mesenteric $CFTR^{+/+}$ 240±11 μm (n=8), mesenteric $CFTR^{-/-}$ 301±34 μm (n=6), P=NS. In **A** and **B**, *$P<0.05$ relative to control; +$P<0.05$ relative to S1P for multiple, unpaired comparisons; in **C** through **E**, *$P<0.05$ after 2-way repeated-measures ANOVA; in **F** and **G**, *$P<0.05$ relative to the $CFTR^{+/+}$ genotype after 2-way ANOVA.

level of FITC-S1P uptake, which was enhanced by stable expression of $CFTR^{wt}$ (Figure 1E; the absolute values for all normalized FITC-S1P uptake data are supplied in Table I in the online-only Data Supplement). In baby hamster kidney cells stably expressing a temperature-sensitive CFTR mutant ($CFTR^{\Delta F508}$), FITC-S1P uptake could only be increased if culture conditions permitted proper membrane localization of CFTR (27°C; Figure 1F).[18] Under conditions causing retention of CFTR in the endoplasmic reticulum (37°C for 24 hours),[18] FITC-S1P uptake was not enhanced by the expression of $CFTR^{\Delta F508}$ (Figure 1F).

CFTR Modulates Effects of S1P on Cells and Vessels

We next explored whether CFTR-dependent S1P transport affects 2 well-documented receptor-dependent responses to exogenous S1P.[3,19] At the cellular level, VSMCs derived from wild-type ($CFTR^{+/+}$) mesenteric arteries possessed a higher rate of proliferation than those isolated from CFTR knockout mice ($CFTR^{-/-}$; see control bars in Figure 2A versus 2B; $P<0.05$). Although treatment with S1P (100 nmol/L) inhibited cell proliferation in both genotypes, pharmacological inhibition of CFTR only enhanced the

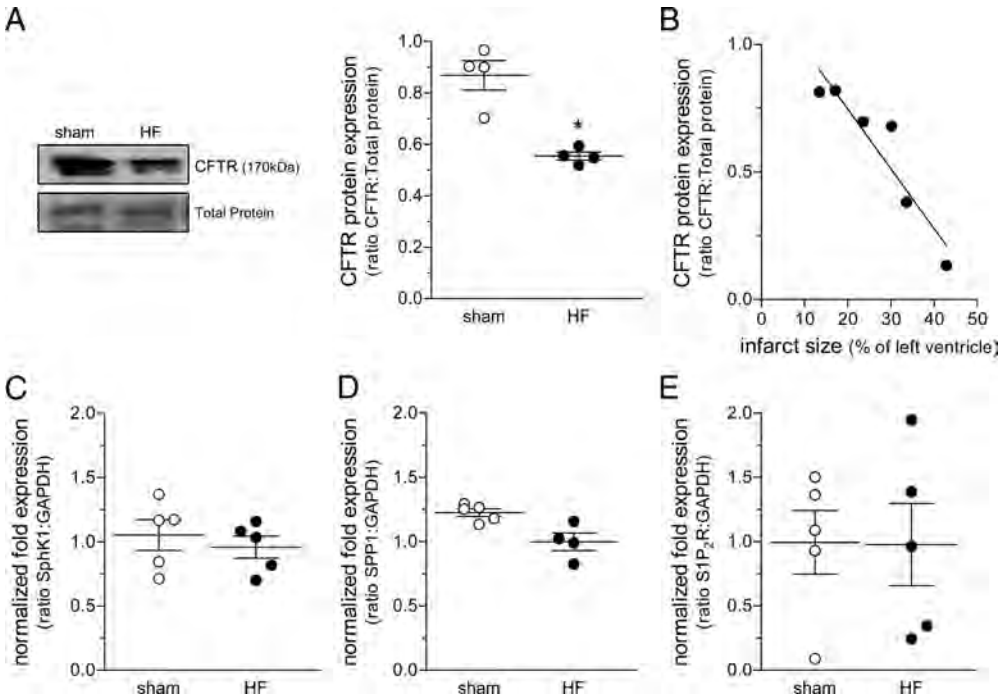

Figure 3. Heart failure (HF) downregulates the cystic fibrosis transmembrane conductance regulator (CFTR) but not sphingosine-1-phosphate (S1P) signaling components. HF (4–6 weeks after myocardial infarction) is associated with the downregulation of posterior cerebral artery CFTR protein expression (n=4) (**A**), which negatively correlated with the extent of the myocardial infarction (**B**). **C** through **E,** HF does not affect the mRNA expression of mesenteric artery sphingosine kinase 1 (SphK1; n=12), S1P phosphohydrolase 1 (SPP1; n=7), or the $S1P_2$ receptor subtype ($S1P_2R$; n=6). *$P<0.05$ for single, unpaired comparisons.

antiproliferative effects of S1P in $CFTR^{+/+}$ cells (Figure 2A and 2B), indicating target specificity of CFTR(inh)-172 and supporting the ability of CFTR to limit S1P-dependent effects.

At the organ level, dose-dependent S1P vasoconstriction of mouse PCAs was more potent in $CFTR^{-/-}$ versus $CFTR^{+/+}$ PCAs (Figure 2C). Importantly, $CFTR^{-/-}$ and $CFTR^{+/+}$ PCAs did not differ in their vasomotor responses to phenylephrine (Figure 2D) or acetylcholine (Figure 2E).

To assess the functional relevance of CFTR to the regulation of endogenous S1P signaling, we examined pressure-induced myogenic vasoconstriction, a complex integrated response modulated prominently by S1P.[2] PCAs isolated from $CFTR^{-/-}$ mice displayed stronger myogenic vasoconstriction at all transmural pressures >40 mm Hg (ie, 60–100 mm Hg) compared with PCAs from $CFTR^{+/+}$ littermate controls (Figure 2F). These effects were not limited to cerebral vessels because mesenteric arteries displayed similar results (Figure 2G). To confirm the full dependence of myogenic responses on S1P signaling, pressure-induced vasoconstriction in both cerebral and mesenteric $CFTR^{-/-}$ vessels was abolished by the putative $S1P_2$ receptor antagonist JTE013 (Figure 2F and 2G).

CFTR Expression Is Diminished in HF

Alterations in S1P signaling are common to several pathological processes. Indeed, we have demonstrated recently that mesenteric and cremasteric artery myogenic responses are significantly enhanced in a post–myocardial infarction model of HF as a result of augmented S1P signaling.[4] Consistent with an inverse relationship between CFTR and S1P signaling, we found marked reductions in CFTR mRNA and protein in PCAs isolated from mice with HF (4–6 weeks after myocardial infarction) versus sham-operated controls (Figure 3A and Figure IIIA in the online-only Data Supplement). Similar reductions in CFTR mRNA (28±11%; n=15; $P<0.05$) and protein (42±5%; n=7; $P<0.05$) were observed in mesenteric arteries isolated from mice with HF (Figure IIIB and IIIC in the online-only Data Supplement). In both vascular beds, CFTR expression correlated negatively with infarct size (Figure 3B and Figure IV in the online-only Data Supplement). As shown in Figure 3C through 3E, HF did not affect expression levels of sphingosine kinase 1, SPP1, or the $S1P_2$ receptor mRNA.

Expression and Localization of CFTR Are Regulated by TNF-α

Because HF is known to increase TNF-α[20–22] and TNF-α is known to augment S1P signaling,[23–25] we next explored whether TNF-α underlies reduced expression levels of CFTR in HF. As we have demonstrated previously,[4] mice with HF displayed evidence of fluid retention and organ congestion (manifested as increased body, heart, lung, and liver weights and an increase in the ratio of heart to body weight) and decreased cardiac function (Table II in the online-only Data Supplement).

Although initiating in vivo etanercept treatment (which sequesters TNF-α) within hours of LAD ligation did not alter infarct size (Figure V in the online-only Data Supplement), it ameliorated the effects of HF on organ weight and all cardiac function parameters except for left ventricular end-systolic and -diastolic pressures (Table II in the online-only Data

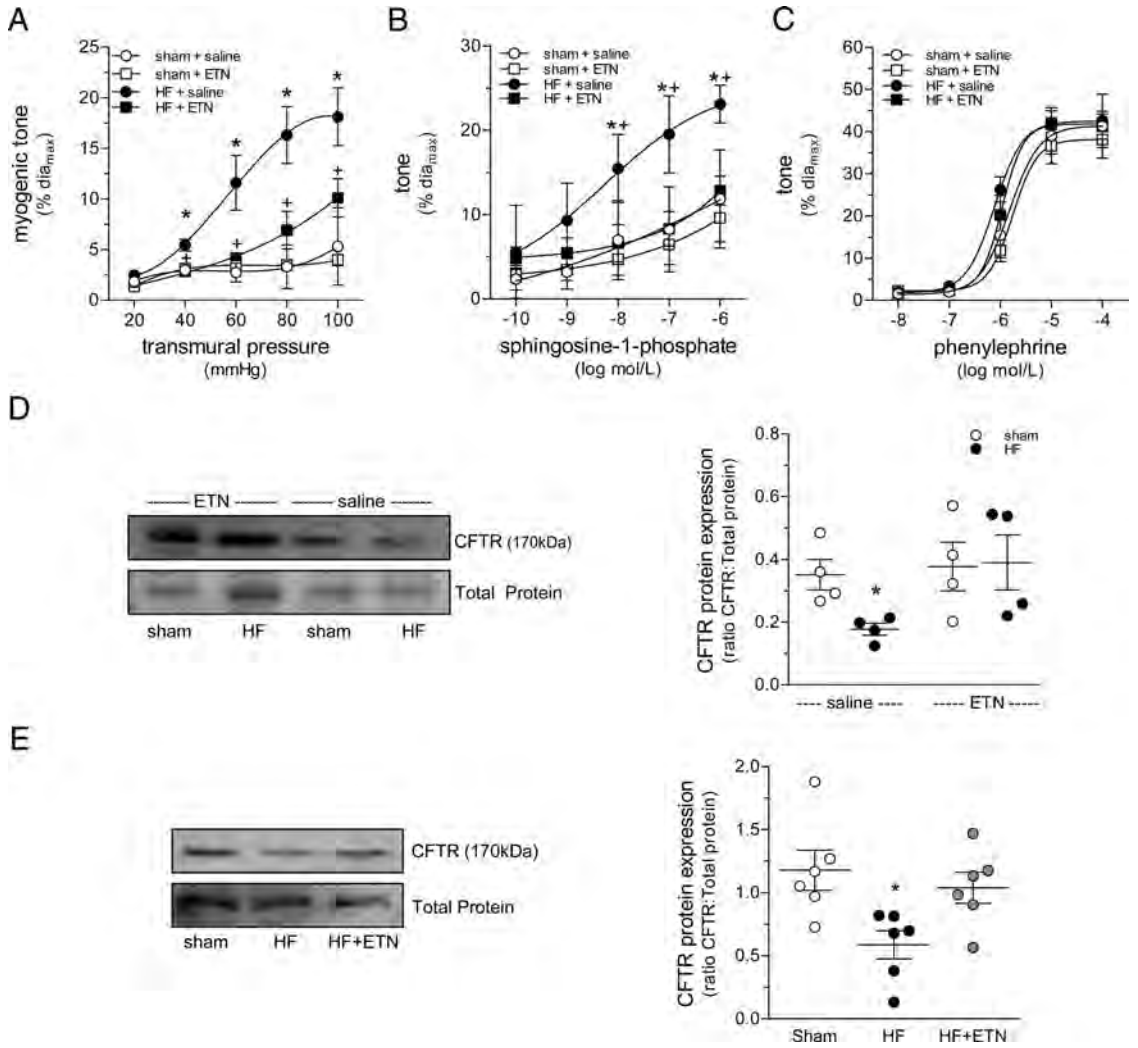

Figure 4. Heart failure (HF) alters myogenic tone, sphingosine-1-phosphate signaling, and cystic fibrosis transmembrane conductance regulator (CFTR) expression by a tumor necrosis factor-α–dependent mechanism. Myogenic tone (**A**) and sphingosine-1-phosphate–stimulated vasoconstriction (**B**) are augmented in posterior cerebral arteries isolated from saline-treated wild-type mice with HF. Sequestration of tumor necrosis factor-α via systemic etanercept (ETN) treatment (initiated immediately after the left anterior descending artery ligation procedure) abolishes these HF-mediated enhancements. Neither HF nor etanercept treatment affects posterior cerebral artery responses to phenylephrine (**C**). In all experiments in **A** through **C**: n=6 for sham+saline; n=5 for HF+saline; n=10 for sham+etanercept; and n=7 for HF+etanercept. Maximal vessel diameters at 45 mm Hg (dia$_{max}$) were 172±4, 172±2, 180±3, and 174±8 μm, respectively (P=NS). The HF-associated downregulation of posterior cerebral artery CFTR protein expression is prevented by immediate (n=4) (**D**) and reversed by delayed (n=6) etanercept treatment (**E**). In **A** through **C**, *P<0.05 relative to the sham+saline group; +significant difference between HF+saline and HF+etanercept after 2-way repeated-measures ANOVA; in **D** and **E**, *P<0.05 for unpaired comparisons with the respective sham control.

Supplement). At the vascular level, this treatment protocol normalized myogenic tone and vasomotor responses to exogenous S1P and prevented CFTR downregulation (Figure 4). Neither HF nor etanercept treatment affected vasomotor responses to phenylephrine (Figure 4C), indicating specific effects on S1P signaling. To assess reversibility, we delayed etanercept treatment (ie, initiated a 2-week treatment at 6 weeks post-LAD ligation) and observed normalized CFTR expression (Figure 4E).

In accordance with the TNF-α sequestration results, HF failed to augment myogenic tone (Figure 5A) and vasomotor responses to S1P (Figure 5B) in PCAs isolated from TNF-α knockout ($TNF^{-/-}$) mice; intriguingly, phenylephrine responses in $TNF^{-/-}$ PCAs were enhanced at the 0.1- and 1-μmol/L concentration in HF (Figure 5C). CFTR protein expression in the PCA did not change in HF (Figure 5D), which indicates that the CFTR downregulation observed in wild-type mice depends on TNF-α signaling. Similar observations for all parameters were made for mesenteric arteries isolated from $TNF^{-/-}$ mice (Figure VI in the online-only Data Supplement).

Primary mouse VSMCs exposed to TNF-α (10 ng/mL, 24 hours) showed reductions in CFTR mRNA (Figure VII in the online-only Data Supplement) and protein (Figure 6A) expression, with a concomitant reduction in their uptake of FITC-S1P (Figure 6B). The TNF-α–mediated effects on CFTR expression and FITC-S1P uptake fully recovered within 24 hours after the removal of TNF-α (Figure 6C and 6D). Of note, TNF-α induced a rapid decline in CFTR expression ($t_{1/2}$=6.5 hours, with significant differences ver-

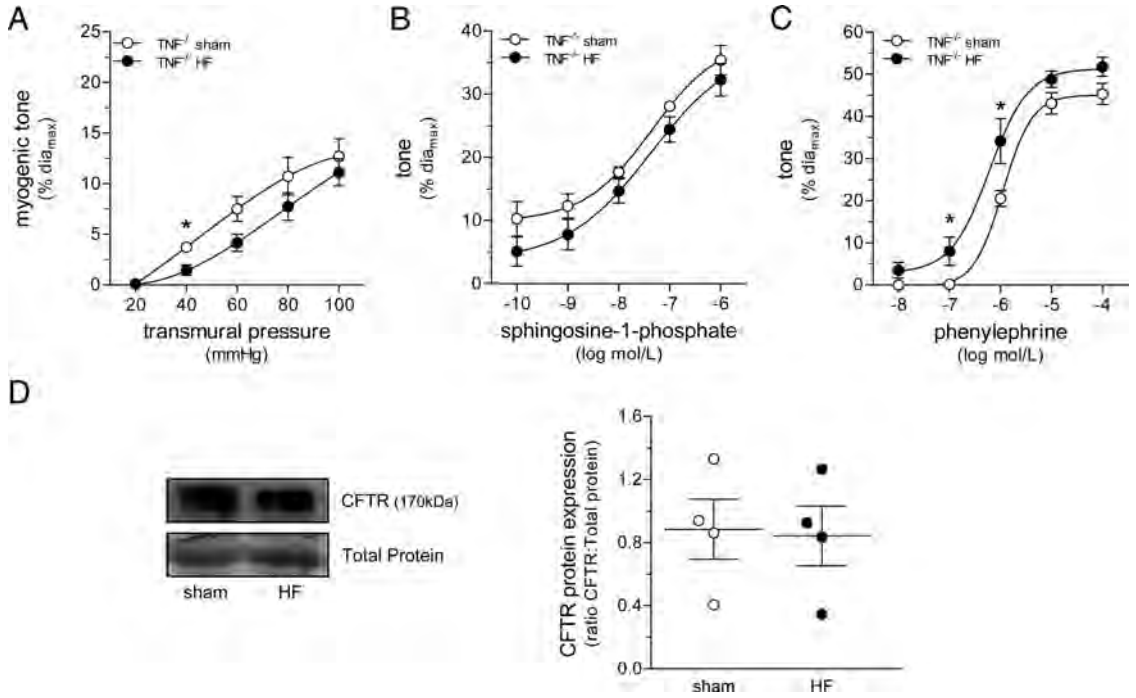

Figure 5. In posterior cerebral arteries isolated from tumor necrosis factor (TNF)$^{-/-}$ mice, heart failure (HF) failed to enhance myogenic tone (**A**) and sphingosine-1-phosphate–stimulated vasoconstriction (**B**), although responses to phenylephrine (**C**) were enhanced at the 1-μmol/L concentration. In all experiments displayed in **A** through **C**: TNF$^{-/-}$ sham maximal diameter at 45 mm Hg (dia$_{max}$)=155±4 μm, n=5; TNF$^{-/-}$ HF dia$_{max}$=158±5 μm, n=7. **D,** Genetic deletion of TNF-α prevented the HF-associated downregulation of posterior cerebral artery cystic fibrosis transmembrane conductance regulator (CFTR) protein expression (n=4 for both groups). In **A** through **C**, *P<0.05 after 2-way repeated-measures ANOVA; in **D**, *P<0.05 for unpaired comparison.

sus control by 9 hours; Figure 6E). A subsequent analysis of the "B" (immature, nonglycosylated CFTR; 165 kDa) and "C" bands (mature, glycosylated CFTR; 170 kDa)[26,27] indicated a loss of the mature form of CFTR (band C), which did not appear to result from reduced expression/maturation (band B; Figure 6E). Assessment of membrane and intracellular fractions indicated a decline in membrane-associated CFTR without intracellular accumulation, consistent with the operation of a degrading mechanism (Figure 6F).

Brain, Heart, and Lung Tissues Also Show a HF-Induced, TNF-α–Dependent Downregulation of CFTR Expression

HF reduces CFTR protein expression in the brain (by 41±3%; n=3), heart (by 18±1%; n=4–5), and lung (by 34±4%; n=4–8); systemic TNF-α sequestration with etanercept (treatment initiated immediately after the LAD ligation) prevents this downregulation (Figure 7A through 7C). Staining of lung slices with a CFTR antibody localized the majority of CFTR expression in terminal bronchioli to the epithelium (Figure 7D).[28] HF significantly reduces bronchial epithelia CFTR expression (by 34%; n=4; Figure 7E and 7F), a result that matches well with the Western blot data displayed in Figure 7C.

Discussion

The rheostat between S1P synthesis[29] and degradation[3] importantly contributes to the control of myogenic tone in resistance arteries. As an intrinsic, smooth muscle cell–dependent response to alterations in transmural pressure, myogenic tone is central to the local autoregulation of tissue perfusion and, at the systemic level, influences mean arterial pressure by dictating the magnitude of total peripheral resistance. A failure to adequately control the S1P rheostat within the microcirculation would therefore have significant detrimental vascular effects, evident at both the local and systemic levels.

We have demonstrated recently that SPP1 degrades extracellular S1P and thus is a physiologically relevant, endogenous regulator of myogenic tone.[3] However, the predominant intracellular localization of SPP1 necessitates an import mechanism in order for SPP1 to exert is regulatory function. This potentially imposes the transport process (ie, the mechanism shuttling extracellular S1P across the plasma membrane for degradation by SPP1) as the key regulatory and rate-limiting step in the S1P degradation chain. Indeed, the fact that there are few known regulators of SPP1 activity supports the view that the transporter, rather than SPP1, is the primary site of S1P degradation control. Previous investigations by us[3] and others[9] provide indirect evidence implicating CFTR in this transport process.

The present investigation identifies a direct pathophysiological link between CFTR and S1P signaling and introduces a novel, broadly applicable paradigm that resolves the issue of the manner in which extracellular S1P is ultimately degraded by intracellular S1P phosphatases. Within the S1P degradation pathway, CFTR acts as a molecular gatekeeper that is well positioned to regulate the entire process. Because S1P signaling plays a critical role in virtually every cell type and is known to be altered in several pathological

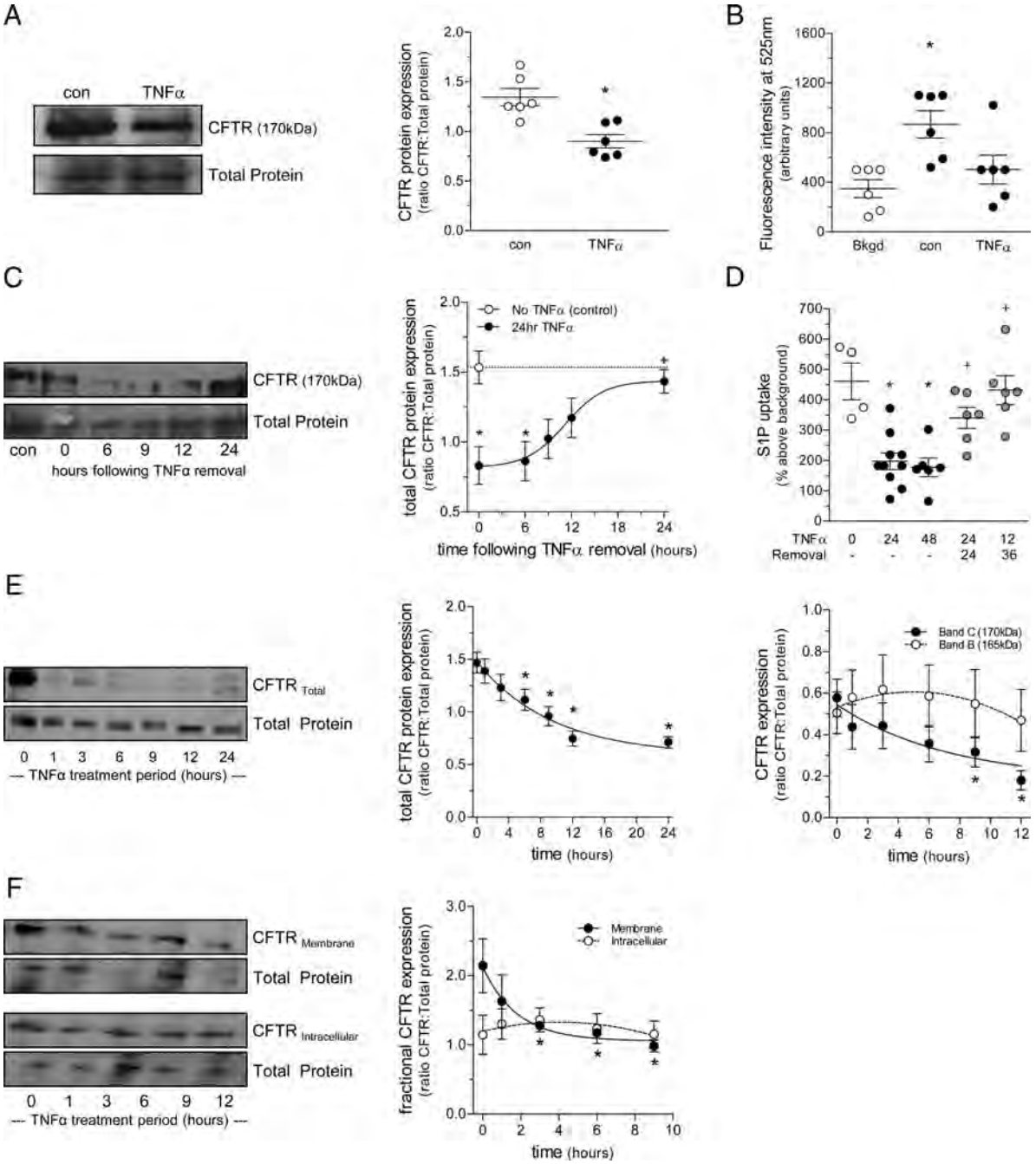

Figure 6. Tumor necrosis factor-α (TNF-α) downregulates cystic fibrosis transmembrane conductance regulator (CFTR) expression and stimulates a reduction in plasma membrane–associated CFTR. **A**, TNF-α (10 ng/mL; 24 hours) stimulates the downregulation of mesenteric vascular smooth muscle cell CFTR protein expression (n=6), with (**B**) a concomitant reduction in fluorescein isothiocyanate–sphingosine-1-phosphate (S1P) uptake (n=6). Both the reduced CFTR expression (n=4) (**C**) and attenuated fluorescein isothiocyanate–S1P uptake (n=4–10) (**D**) were completely reversed 24 hours after TNF-α washout. **E**, TNF-α treatment (10 ng/mL) stimulates a steady decline in CFTR protein expression (n=4). Analysis of the 165-kDa (immature, nonglycosylated CFTR; band B) and 170-kDa (mature, glycosylated CFTR; band C) bands indicated that only the mature form of CFTR declined. **F**, Analysis of plasma membrane and intracellular fractions (n=6) indicated that membrane-associate CFTR was reduced without a concomitant accumulation of intracellular-associated CFTR. In **A** and **B**, **P*<0.05 for unpaired comparisons with control (con)/background (Bkgd); in **C** through **F**, **P*<0.05 for multiple, unpaired comparisons with the control value at time=0 hours; +*P*<0.05 for difference between pre–TNF-α removal and TNF-α removal.

settings, it is conceivable that CFTR dysregulation contributes to a range of immunologic,[10] cardiovascular,[11] and oncogenic[12] disorders with an S1P component. In this regard, our paradigm positions CFTR as a potential therapeutic target for these conditions.

Our investigation has also improved our understanding of mechanisms that regulate S1P signaling in resistance artery VSMCs. A traditional viewpoint favors increased S1P synthesis as the primary means of elevating S1P levels; although energy intensive, this mechanism clearly operates during

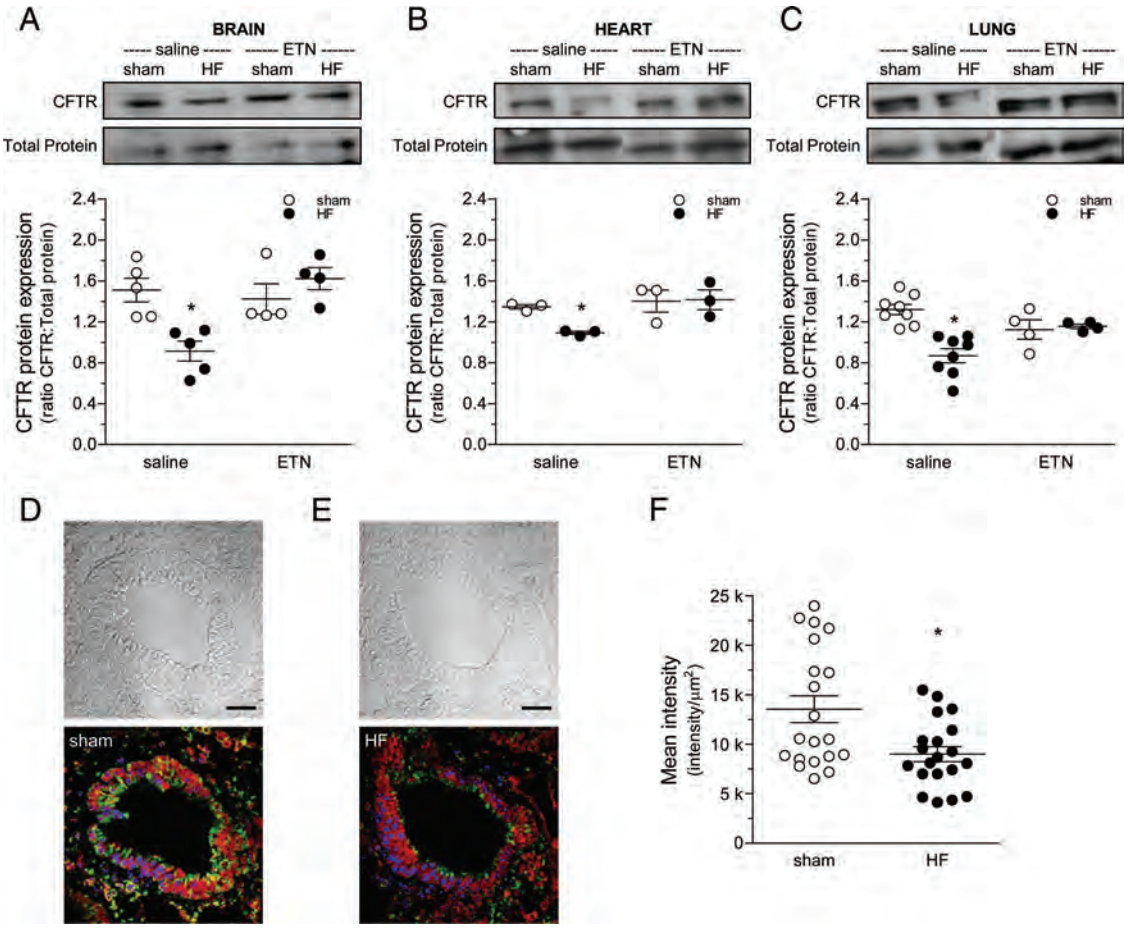

Figure 7. Heart failure (HF) downregulates cystic fibrosis transmembrane conductance regulator (CFTR) protein expression in brain, heart, and lung. HF (4–6 weeks after myocardial infarction) is associated with the downregulation of CFTR protein expression in brain (**A**), heart (**B**), and lung (**C**); sequestration of tumor necrosis factor-α via systemic etanercept treatment (ETN; initiated immediately after the left anterior descending artery ligation procedure) abolishes this downregulation. *$P<0.05$ for multiple, unpaired comparisons with the sham+saline control groups; n=4 to 5 for brain; n=3 for heart; and n=4 to 8 for lung. **D** and **E**, Representative images of lung slices from HF mice (**E**; n=4) and sham-operated controls (**D**; n=4) that are stained for CFTR (green), nuclear factor-κB (cytosolic marker; red), and nuclei (Hoechst 33258; blue). HF significantly reduces epithelial CFTR expression in terminal bronchioli (**F**). *$P<0.05$ for unpaired comparisons between sham and HF groups; images are representative of at least 20 slices per group (ie, 5 per animal).

acute myogenic vasoconstriction responses.[29] In contrast, enhancing S1P signaling through limited uptake/degradation via CFTR enables a system to maintain high levels of S1P signaling at a constant synthesis rate, with minimal energy cost. Indeed, our data demonstrate the effectiveness of inhibiting S1P degradation, and we speculate that this may be the preferred mechanism for sustained elevations of S1P signaling in chronic conditions such as HF.

In the present study, we demonstrate that perturbation of CFTR expression or localization significantly alters S1P signaling. Reducing plasma membrane CFTR abundance (genomic deletion [$CFTR^{-/-}$], downregulation after TNF-α treatment, and intracellular retention [$CFTR^{\Delta F508}$]) augmented S1P signaling. In the case of the $CFTR^{\Delta F508}$ mutant, we confirm that in order to transport extracellular S1P, CFTR must reside within the plasma membrane.

On the basis of the relationship between CFTR and S1P signaling we establish here, we would expect that the most widely recognized pathology associated with CFTR dysfunction, cystic fibrosis, should encompass vascular effects mediated by enhanced S1P signaling (in addition to or in conjunction with effects related to the other functions of CFTR, eg, chloride transport). Although cystic fibrosis is associated with cardiac impairment,[30,31] it is not clinically associated with hypertension, a systemic effect that would be predicted as a consequence of S1P-dependent augmentation of myogenic tone and hence peripheral resistance. However, mean arterial pressure measurements integrate several factors and mechanisms (eg, blood volume, cardiac output, total peripheral resistance). In addition to cardiac dysfunction,[30,31] patients with cystic fibrosis are known to have increased sweat salt loss[32]; both are confounding factors that could ameliorate the effects of increased resistance artery tone. Nevertheless, our findings align well with previous studies reporting altered lipid metabolism in patients with cystic fibrosis (eg, accumulation of ceramide,[33] a lipid mediator involved in the sphingolipid rheostat[1]).

To date, very little effort has been made to investigate S1P signaling in clinical or experimental cystic fibrosis. This may reflect the fact that the importance of CFTR in controlling S1P bioavailability has been largely underestimated. The present investigation clearly demonstrates that the genetic

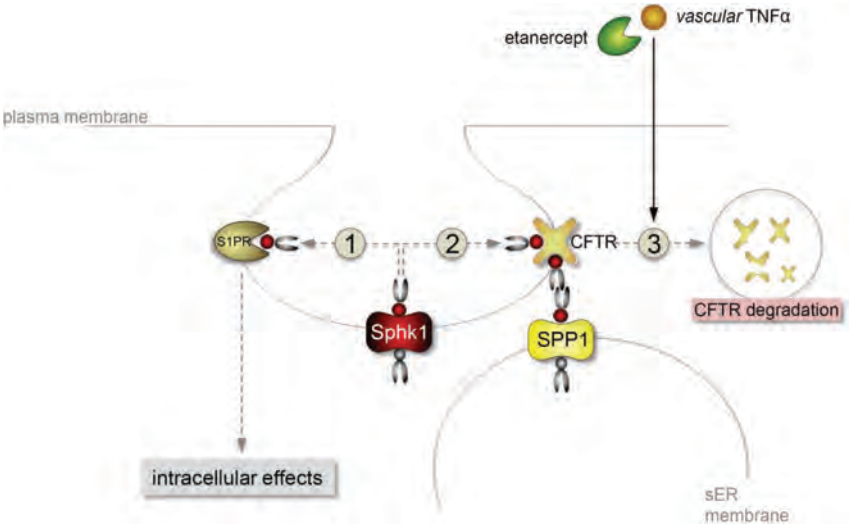

Figure 8. Schematic representation of the proposed relationship between cystic fibrosis transmembrane conductance regulator (CFTR) and sphingosine-1-phosphate (S1P) signaling. S1P produced by sphingosine kinase 1 (Sphk1) is released to the extracellular compartment, where it (1) activates S1P receptor (S1PR)–dependent signaling pathways or (2) is transported by CFTR across the plasma membrane for degradation by S1P phosphohydrolase 1 (SPP1). During heart failure, tumor necrosis factor-α (TNF-α) stimulates the downregulation of CFTR (3), thus inhibiting S1P degradation and concomitantly enhancing S1P receptor signaling. sER indicates smooth endoplasmic reticulum.

deletion of CFTR results in a marked enhancement of S1P-stimulated vasoconstriction and myogenic tone, observations that corroborate previous results utilizing a chemical CFTR inhibitor.[3] In the case of myogenic vasoconstriction, the enhancement was observed in 2 structurally and functionally distinct artery types (ie, mesenteric and cerebral resistance arteries), suggesting that this enhancement is not confined to 1 specific artery subtype. Taken together, our observations support the premise that CFTR is an integral element determining resistance artery homeostasis, with direct relevance under both physiological and potentially pathophysiological conditions.

CFTR regulation, which includes expression, localization, and gating, is highly dynamic; changes in CFTR function/expression could represent an important underlying component of several disease processes. In particular, the inflammatory mediator TNF-α is a negative regulator of CFTR,[34–37] which tacitly involves CFTR in conditions that possess an inflammatory component. Remarkably, we have demonstrated previously that TNF-α augments resistance artery contractile function via an S1P-dependent mechanism, both when applied exogenously ex vivo[5,38] and under the more relevant systemic inflammatory setting of HF.[5] Although we[38] and others[39] have also documented TNF-α–dependent activation of sphingosine kinase 1, this mechanism alone cannot explain the leftward shift in the S1P dose-response relationship observed (Figure 4B). In fact, the augmented responses to exogenous S1P suggest either increased $S1P_2$ receptor function or impairment of S1P degradation as the underlying cause. In the absence of alterations to $S1P_2$ or SPP1 expression, the current data favor reduced CFTR expression and/or function as the primary underlying mechanism.

Our results suggest that TNF-α reversibly controls CFTR expression by both genomic and nongenomic mechanisms. In the short term, we observe a steady decline of membrane-associated CFTR, without intracellular accumulation (Figure 6F) or perturbation in the levels of immature CFTR (Figure 6E). This indicates that membrane-associated CFTR is degraded as opposed to sequestered. After 24 hours, reductions in CFTR mRNA are observed, suggesting genomic effects on transcription or mRNA stability.

The suppression of CFTR expression in concert with limiting membrane abundance occurs on a time scale that is compatible with both short- and long-term regulation of CFTR function. In our chronic model of HF, we observe a TNF-α–dependent (ie, etanercept-sensitive) downregulation of CFTR that correlates with the enhancement of S1P-dependent effects on microvascular tone and with a reported reduction in cerebral blood flow.[5] Interrupting TNF-α signaling immediately after LAD ligation prevents the downregulation of CFTR, which subsequently enhances S1P signaling. Interrupting TNF-α signaling at later time points, after HF is fully established, restores CFTR expression and microvascular S1P signaling.

The same paradigm was observed in whole-organ lysates from brain, heart, and lung, which consistently demonstrated etanercept-sensitive CFTR downregulation in HF (Figure 7). The fact that HF downregulates CFTR expression in terminal bronchioli epithelial cells, which differ from vascular smooth muscle in terms of both function and developmental origin, elevates the significance of our findings beyond that of the microvascular field. It is tempting to speculate that TNF-α–induced CFTR downregulation (see scheme in Figure 8) is a global response and a key underlying component driving multiorgan dysfunction in HF.

In summary, CFTR represents a bottleneck within the S1P degradation pathway that therefore controls S1P signaling. CFTR dysfunction therefore perturbs S1P signaling and, as such, could represent an underlying cause of pathogenic changes in S1P signaling (ie, CFTR is an upstream target in the disease process). In the present study, we present data suggesting that the reversible downregulation of CFTR enhances microvascular reactivity in HF, a critical determinant of disease progression. On the basis of this investigation, we conclude that CFTR represents an unexplored therapeutic target for conditions related to altered S1P signaling.

Sources of Funding

We gratefully acknowledge the following funding support: operating and infrastructure grants from the Canadian Institutes of Health

Research (to Dr Bolz; MOP-84402); Heart and Stroke Foundation of Ontario (to Dr Bolz; NA7064); Canadian Foundation for Innovation and Ontario Research Fund (to Dr Bolz; 11810); Canadian Stroke Network (to Dr Bolz); start-up funding from the University of Toronto (to Dr Bolz); a Heart and Stroke Foundation of Ontario New Investigator Award (to Dr Bolz); and a Heart and Stroke Foundation of Ontario Career Investigator Award (to Dr Husain; CI5503). Both Jeffrey T. Kroetsch and Meghan Sauvé hold graduate scholarships (stipend support) awarded by the Heart and Stroke/Richard Lewar Centre of Excellence for Cardiovascular Research.

Disclosures

None.

References

1. Spiegel S, Milstien S. Sphingosine-1-phosphate: an enigmatic signalling lipid. *Nat Rev Mol Cell Biol*. 2003;4:397–407.
2. Bolz SS, Vogel L, Sollinger D, Derwand R, Boer C, Pitson SM, Spiegel S, Pohl U. Sphingosine kinase modulates microvascular tone and myogenic responses through activation of rhoA/rho kinase. *Circulation*. 2003;108:342–347.
3. Peter BF, Lidington D, Harada A, Bolz HJ, Vogel L, Heximer S, Spiegel S, Pohl U, Bolz SS. Role of sphingosine-1-phosphate phosphohydrolase 1 in the regulation of resistance artery tone. *Circ Res*. 2008;103:315–324.
4. Hoefer J, Azam MA, Kroetsch JT, Poi HL, Momen MA, Voigtlaender-Bolz J, Scherer EQ, Meissner A, Bolz SS, Husain M. Sphingosine-1-phosphate-dependent activation of p38 MAPK maintains elevated peripheral resistance in heart failure through increased myogenic vasoconstriction. *Circ Res*. 2010;107:923–933.
5. Yang J, Meissner A, Lidington D, Bolz SS. TNF enhances cerebral microvascular tone during congestive heart failure via activation of sphingosine kinase 1. *Can J Cardiol*. 2009;25:179.
6. Pyne S, Lee SC, Long J, Pyne NJ. Role of sphingosine kinases and lipid phosphate phosphatases in regulating spatial sphingosine 1-phosphate signalling in health and disease. *Cell Signal*. 2009;21:14–21.
7. Le Stunff H, Peterson C, Liu H, Milstien S, Spiegel S. Sphingosine-1-phosphate and lipid phosphohydrolases. *Biochim Biophys Acta*. 2002;1582:8–17.
8. Le Stunff H, Galve-Roperh I, Peterson C, Milstien S, Spiegel S. Sphingosine-1-phosphate phosphohydrolase in regulation of sphingolipid metabolism and apoptosis. *J Cell Biol*. 2002;158:1039–1049.
9. Boujaoude LC, Bradshaw-Wilder C, Mao C, Cohn J, Ogretmen B, Hannun YA, Obeid LM. Cystic fibrosis transmembrane regulator regulates uptake of sphingoid base phosphates and lysophosphatidic acid: modulation of cellular activity of sphingosine 1-phosphate. *J Biol Chem*. 2001;276:35258–35264.
10. Nixon GF. Sphingolipids in inflammation: pathological implications and potential therapeutic targets. *Br J Pharmacol*. 2009;158:982–993.
11. Skoura A, Hla T. Regulation of vascular physiology and pathology by the S1P2 receptor subtype. *Cardiovasc Res*. 2009;82:221–228.
12. Pyne NJ, Pyne S. Sphingosine 1-phosphate and cancer. *Nat Rev Cancer*. 2010;10:489–503.
13. Lorenz JN, Arend LJ, Robitz R, Paul RJ, MacLennan AJ. Vascular dysfunction in S1P2 sphingosine 1-phosphate receptor knockout mice. *Am J Physiol*. 2007;292:R440–R446.
14. Coussin F, Scott RH, Wise A, Nixon GF. Comparison of sphingosine 1-phosphate–induced intracellular signaling pathways in vascular smooth muscles: differential role in vasoconstriction. *Circ Res*. 2002;91:151–157.
15. Marino MW, Dunn A, Grail D, Inglese M, Noguchi Y, Richards E, Jungbluth A, Wada H, Moore M, Williamson B, Basu S, Old LJ. Characterization of tumor necrosis factor-deficient mice. *Proc Natl Acad Sci U S A*. 1997;94:8093–8098.
16. Snouwaert JN, Brigman KK, Latour AM, Malouf NN, Boucher RC, Smithies O, Koller BH. An animal model for cystic fibrosis made by gene targeting. *Science*. 1992;257:1083–1088.
17. Peest U, Sensken SC, Andreani P, Hanel P, Van Veldhoven PP, Graler MH. S1P-lyase independent clearance of extracellular sphingosine 1-phosphate after dephosphorylation and cellular uptake. *J Cell Biochem*. 2008;104:756–772.
18. French PJ, van Doorninck JH, Peters RH, Verbeek E, Ameen NA, Marino CR, de Jonge HR, Bijman J, Scholte BJ. A delta F508 mutation in mouse cystic fibrosis transmembrane conductance regulator results in a temperature-sensitive processing defect in vivo. *J Clin Invest*. 1996;98:1304–1312.
19. Wamhoff BR, Lynch KR, Macdonald TL, Owens GK. Sphingosine-1-phosphate receptor subtypes differentially regulate smooth muscle cell phenotype. *Arterioscler Thromb Vasc Biol*. 2008;28:1454–1461.
20. Torre-Amione G. Immune activation in chronic heart failure. *Am J Cardiol*. 2005;95:3C–8C.
21. Doyama K, Fujiwara H, Fukumoto M, Tanaka M, Fujiwara Y, Oda T, Inada T, Ohtani S, Hasegawa K, Fujiwara T, Sasayama S. Tumour necrosis factor is expressed in cardiac tissues of patients with heart failure. *Int J Cardiol*. 1996;54:217–225.
22. Koller-Strametz J, Pacher R, Frey B, Kos T, Woloszczuk W, Stanek B. Circulating tumor necrosis factor-alpha levels in chronic heart failure: relation to its soluble receptor II, interleukin-6, and neurohumoral variables. *J Heart Lung Transplant*. 1998;17:356–362.
23. Xia P, Gamble JR, Rye KA, Wang L, Hii CS, Cockerill P, Khew-Goodall Y, Bert AG, Barter PJ, Vadas MA. Tumor necrosis factor-alpha induces adhesion molecule expression through the sphingosine kinase pathway. *Proc Natl Acad Sci U S A*. 1998;95:14196–14201.
24. Radeff-Huang J, Seasholtz TM, Chang JW, Smith JM, Walsh CT, Brown JH. Tumor necrosis factor-alpha-stimulated cell proliferation is mediated through sphingosine kinase-dependent Akt activation and cyclin D expression. *J Biol Chem*. 2007;282:863–870.
25. Donati C, Nincheri P, Cencetti F, Rapizzi E, Farnararo M, Bruni P. Tumor necrosis factor-alpha exerts pro-myogenic action in C2C12 myoblasts via sphingosine kinase/S1P2 signaling. *FEBS Lett*. 2007;581:4384–4388.
26. Wang Y, Loo TW, Bartlett MC, Clarke DM. Additive effect of multiple pharmacological chaperones on maturation of CFTR processing mutants. *Biochem J*. 2007;406:257–263.
27. Thibodeau PH, Richardson JM III, Wang W, Millen L, Watson J, Mendoza JL, Du K, Fischman S, Senderowitz H, Lukacs GL, Kirk K, Thomas PJ. The cystic fibrosis-causing mutation deltaF508 affects multiple steps in cystic fibrosis transmembrane conductance regulator biogenesis. *J Biol Chem*. 2010;285:35825–35835.
28. Jiang Q, Engelhardt JF. Cellular heterogeneity of CFTR expression and function in the lung: implications for gene therapy of cystic fibrosis. *Eur J Hum Genet*. 1998;6:12–31.
29. Lidington D, Peter BF, Meissner A, Kroetsch JT, Pitson SM, Pohl U, Bolz SS. The phosphorylation motif at serine 225 governs the localization and function of sphingosine kinase 1 in resistance arteries. *Arterioscler Thromb Vasc Biol*. 2009;29:1916–1922.
30. Labombarda F, Pellissier A, Ellafi M, Creveuil C, Ribault V, Laurans M, Guillot M, Bergot E, Grollier G, Milliez P, Zalcman G, Saloux E. Myocardial strain assessment in cystic fibrosis. *J Am Soc Echocardiogr*. 2011;24:1037–1045.
31. Koelling TM, Dec GW, Ginns LC, Semigran MJ. Left ventricular diastolic function in patients with advanced cystic fibrosis. *Chest*. 2003;123:1488–1494.
32. Super M, Irtiza-Ali A, Roberts SA, Schwarz M, Young M, Smith A, Roberts T, Hinks J, Heagerty A. Blood pressure and the cystic fibrosis gene: evidence for lower pressure rises with age in female carriers. *Hypertension*. 2004;44:878–883.
33. Teichgräber V, Ulrich M, Endlich N, Riethmuller J, Wilker B, De Oliveira-Munding CC, van Heeckeren AM, Barr ML, von Kürthy G, Schmid KW, Weller M, Tummler B, Lang F, Grassme H, Döring G, Gulbins E. Ceramide accumulation mediates inflammation, cell death and infection susceptibility in cystic fibrosis. *Nat Med*. 2008;14:382–391.
34. Baudouin-Legros M, Hinzpeter A, Jaulmes A, Brouillard F, Costes B, Fanen P, Edelman A. Cell-specific posttranscriptional regulation of CFTR gene expression via influence of MAPK cascades on 3′UTR part of transcripts. *Am J Physiol*. 2005;289:C1240–C1250.
35. Nakamura H, Yoshimura K, Bajocchi G, Trapnell BC, Pavirani A, Crystal RG. Tumor necrosis factor modulation of expression of the cystic fibrosis transmembrane conductance regulator gene. *FEBS Lett*. 1992;314:366–370.
36. Bartoszewski R, Rab A, Twitty G, Stevenson L, Fortenberry J, Piotrowski A, Dumanski JP, Bebok Z. The mechanism of cystic fibrosis transmembrane conductance regulator transcriptional repression during the unfolded protein response. *J Biol Chem*. 2008;283:12154–12165.
37. Brouillard F, Bouthier M, Leclerc T, Clement A, Baudouin-Legros M, Edelman A. NF-kappa B mediates up-regulation of CFTR gene expression in Calu-3 cells by interleukin-1beta. *J Biol Chem*. 2001;276:9486–9491.

38. Scherer EQ, Yang J, Canis M, Reimann K, Ivanov K, Diehl CD, Backx PH, Wier WG, Strieth S, Wangemann P, Voigtlaender-Bolz J, Lidington D, Bolz SS. TNF-α enhances microvascular tone and reduces blood flow in the cochlea via enhanced S1P signaling. *Stroke*. 2010;41:2618–2624.

39. Xia P, Wang L, Moretti PA, Albanese N, Chai F, Pitson SM, D'Andrea RJ, Gamble JR, Vadas MA. Sphingosine kinase interacts with TRAF2 and dissects tumor necrosis factor-alpha signaling. *J Biol Chem*. 2002;277:7996–8003.

CLINICAL PERSPECTIVE

This study brings forth the novel concept that changes in vascular cystic fibrosis transmembrane conductance regulator expression underlie the enhancement of vascular tone in heart failure. Our investigation additionally shows that this pathophysiological response is widespread, suggesting that it is a global response that may drive multiorgan dysfunction in heart failure. At the mechanistic level, the cystic fibrosis transmembrane conductance regulator functions as a key regulator of sphingosine-1-phosphate degradation, the modulation of which critically alters myogenic and vascular tone. We conclude that the cystic fibrosis transmembrane conductance regulator represents an unexplored therapeutic target for the improvement of vascular function in heart failure.

SUPPLEMENTAL MATERIAL

SUPPLEMENTAL METHODS

Reagents

Sphingosine-1-phosphate (S1P) was purchased from Biomol International (Plymouth Landing, USA), fluorescein-labeled S1P (FITC-S1P) from Echelon Biosciences (Salt Lake City, USA), JTE013 from Tocris Bioscience (Ellisville, USA) and etanercept from Amgen (Thousand Oaks, USA). Protease inhibitor cocktail tablets (Complete®; used in western blot lysis buffers) were purchased from Roche (Mississauga, Canada). All other chemical reagents were purchased from Sigma-Aldrich (St. Louis, USA). MOPS-buffered salt solution contained [mmol/L]: NaCl 145, KCl 4.7, $CaCl_2$ 3.0, $MgSO_4$ •$7H_2O$ 1.17, NaH_2PO_4 •$2H_2O$ 1.2, pyruvate 2.0, EDTA 0.02, MOPS (3morpholinopropanesulfonic acid) 3.0, and glucose 5.0.

Commercially-available CFTR (clone CF3 mouse monoclonal anti-CFTR; Novus Biologicals, Littleton USA) and GAPDH (clone 9B3 mouse monoclonal anti-GAPDH; Santa Cruz Biotechnology, Santa Cruz, USA) primary antibodies were used for western blotting. These were conjugated with peroxidase-labeled sheep anti-mouse IgG antibody (GE Healthcare; Piscataway, USA) and detected with an "ECL Plus" enhanced chemiluminescence substrates (GE Healthcare) and X-ray film.

$CFTR^{-/-}$ VSMC cells were transfected with GFP-labeled CFTR ($GFP\text{-}CFTR^{wt}$; a gift from Dr. C. Bear, University of Toronto, Canada) using Effectene transfection reagent (Qiagen; Mississauga, Canada), according to the manufacturer's instructions (each 35mm culture dish received 0.4µg of the $GFP\text{-}CFTR^{wt}$ plasmid construct). The cells were transfected overnight; successful transfection was verified by the fluorescent detection of GFP.

Baby Hamster Kidney cells

Naïve baby hamster kidney fibroblast cells (BHK cells), BHK cells stably expressing wild-type CFTR ($CFTR^{wt}$) [1] and BHK cells stably expressing the ΔF508 CFTR mutant ($CFTR^{\Delta F508}$) [1] were generous gifts from Dr. C. Bear (University of Toronto, Canada). Naïve BHK cells were maintained in DMEM/F12 media containing 5% FBS; the media for BHK cells expressing CFTR additionally contained 500µmol/L methotrexate (which activates the CFTR transgene promoter). Cells were maintained under standard culture conditions (37^oC, $5\%CO_2$).

RT-PCR

RNA was isolated using a Qiagen RNeasy® Kit, as per instructions. Using a "Superscript III" kit (Invitrogen Life Technologies; Burlington, Canada), 5µg of total RNA was reverse transcribed with random hexamer primers. The resulting cDNA was diluted to a final volume of 280µl, which was subsequently used as a template for PCR reactions. The PCR protocol, consisted of 40 cycles of 30s denaturation (95^oC); 45s primer annealing (at the primer-specific annealing temperature); and 45s primer extension (72^oC). Resultant PCR products were separated on a 2.5% agarose gel containing ethidium bromide and analyzed by densitometry using publicly available "Image J" software. A list of all primers utilized, their specific annealing temperatures and the expectant amplicon sizes are listed in **Supplemental Table 3**.

Western Blotting

Vessel lysates were prepared by grinding the tissue in lysis buffer containing 25mM Tris (pH6.8), 1% SDS, 10% glycerol, 1mM EDTA, 0.7M β-mercaptoethanol and 25µg/ml protease inhibitor cocktail, followed by freeze-thaw cycles using liquid nitrogen. The resulting lysates were heated to 65^oC for 10 minutes and then centrifuged (30 minutes at 15,000g; 4^oC) to remove insoluble material.

Whole-cell lysates were prepared by lysing cells (6 freeze-thaw cycles using liquid nitrogen followed by room temperature vortexing) in lysis buffer containing 20mM Tris (pH 7.5), 140mM NaCl, 1% NP-40, 10% glycerol, 0.2mM EDTA, 2mM EGTA and 25μg/ml protease inhibitor cocktail. The resulting lysates were centrifuged (30 minutes at 15,000g; 4°C) to remove insoluble material.

Membrane fractions were prepared as previously described [2]. Briefly, confluent VSMC monolayers were lysed (6 freeze-thaw cycles using liquid nitrogen followed by room temperature vortexing) in buffer containing 10mM Tris (pH 7.3), 140mM NaCl, 1% Triton-X-100, 5mM EDTA, 1mM DTT and 25μg/ml protease inhibitor cocktail. The samples were centrifuged (30 minutes at 15,000g; 4°C) to remove insoluble material. The supernatant was then overlayed 1:1 with 3% sucrose and incubated for 5 minutes at room temperature and then 5 minutes at 30°C. Following centrifugation (5 minutes at 2000rpm; 4°C), two phases are evident: a clear phase containing the cytosolic fraction and a translucent phase containing the membrane fraction. The cytosolic fraction (clear phase) was mixed 1:1 with buffer containing 10mM Tris (pH 7.3), 140mM NaCl, 1.5mM KCl, 5mM EDTA, 1mM DTT, and 25μg/ml protease inhibitor cocktail, heated to 65°C for 10 minutes and then centrifuged (30 minutes at 15,000g; 4°C) to remove insoluble material. The membrane fraction was not processed further. Control western blots utilizing membrane (integrin β8) and cytosolic (GAPDH) markers indicated good separation of the plasma membrane and intracellular fractions (**Supplemental Figure 8**).

A standard polyacrylamide gel electrophoresis procedure was utilized to separate the protein samples. Briefly, protein levels were quantified spectrophotometrically using Bradford reagent. Equal amounts of protein were loaded onto either 5% acrylamide gels (for CFTR) or 15% acrylamide gels (for GAPDH), separated electrophoretically and transferred onto PVDF membranes. Immediately following transfer, protein levels on the blot were quantified densitometrically with the rapidly reversible protein stain Ponceau S. After washing the Ponceau stain with distilled water, the membranes were blocked for 60 minutes in 5% non-fat skim milk (in phosphate-buffered saline containing 1% Tween 20 (PBST); 137mM NaCl, 2.7mM KCl, 10mM Na_2HPO_4, 1.76mM K_2HPO_4; pH 7.4) and sequentially incubated with the primary and secondary antibodies. Antibody dilutions were 1:1000 for CFTR, 1:2,000 for GADPH and 1:40,000 for the peroxidase-labeled secondary antibody (all diluted in 2% bovine serum albumin in PBST). A standard chemiluminescence procedure was used to expose X-ray film; developed films were evaluated densitometrically using "Image J" software.

Resolution of the CFTR "C band" (mature, membrane associated; 170kDa [3,4]), the target band for CFTR quantification, requires the 5% acrylamide gel concentration in order to gain sufficient separation from the "B band" (165kDa [3,4]): this precluded the assessment of GAPDH on the same blot, which runs off the gel. Because lysates from cultured cells provided substantial amounts of protein, we were able to compare densitometric ratios derived from a duplicate blot approach (i.e., GADPH:CFTR, from two separate blots) and a single blot approach (i.e., an arbitrary, submaximal band detected by Ponceau S: CFTR, from the same blot). We found that both methods return similar results. All blots using cultured cells were analyzed by both approaches; however the manuscript only presents the duplicate blot approach. Because of the low protein levels available in vessel lysates, only the single blot approach was utilized for these experiments.

VSMC Proliferation Assay

Initially, 10^5 VSMCs were plated and cultured in 35mm diameter chambers for 24hrs. The culture medium was then exchanged for medium containing S1P (100nmol/L), S1P (100nmol/L) + CFTR(inh)-172 (100nmol/L) or no treatment and cultured for 96hrs. The cells were then trypsinized (0.5ml of 0.025% trypsin/0.02% EDTA) for 2 minutes at 37°C in order to detach them from the plates and re-suspended in 1.5ml of medium. Cell counts within aliquots of the resultant suspensions were determined using a Thoma chamber; the total proliferation level was then extrapolated.

Small artery studies:

All functional vessel experiments were conducted in MOPS-buffered saline at 37^{o}C and transmural pressure of 45mmHg, with the exception of myogenic responses (see below). *Vasomotor responses* to phenylephrine (PE; 5µmol/L) and acetylcholine (ACh; 10µmol/L) provided an assessment of vessel viability at the beginning and end of each experiment. PCAs failing to show ≥25% constriction to PE and ≥20% dilation to ACh (in the presence of 5µmol/L PE) were excluded.

Myogenic responses were elicited by step-wise 20mmHg increases in transmural pressure from 20 to 100mmHg. At each pressure step, vessel diameter (dia_{active}) was measured once a steady state was reached (5min). Vessels requiring treatment (50pg/ml TNFα or 1µmol/L JTE013) were incubated with the reagent in MOPS for 30 min at 45mmHg, and myogenic responses were then assessed in the presence of that reagent. Following completion of all dia_{active} measurements, MOPS buffer was replaced with a Ca^{2+}-free version and maximal passive diameter (dia_{max}) was recorded at each pressure step.

Assessment of myocardial infarction:

A standard procedure for determining infarct size was followed [5,6]. Following euthanization, hearts were removed, fixed in 10% formaldehyde and paraffin embedded. Slices (10µm) were stained with hematoxylin and eosin. Infarct size was calculated by comparing the circumferential length of the infarct to the total myocardial length, resulting in a percentage-based index in infarct size.

SUPPLEMENTAL TABLE 1: ***Raw data used to calculate normalized FITC-S1P uptake values***

A

	Naive BHK		BHK + $CFTR^{wt}$		BHK + $CFTR^{\Delta F508}$ 37°C		BHK + $CFTR^{\Delta F508}$ 27°C	
	Background	**FITC-S1P**	**Background**	**FITC-S1P**	**Background**	**FITC-S1P**	**Background**	**FITC-S1P**
Mean	1181	1641	806	2586	1986	2114	1807	2529
SEM	111	142	35	53	51	46	68	148
number	4	4	4	4	7	7	7	7

Shown are the mean fluorescence intensity data (arbitrary units; collected by FACS analysis) that was subsequently normalized and presented as S1P uptake values in Figures 1E and 1F. All FITC-S1P values are significantly higher ($P<0.05$) than their respective background control (unlabeled S1P).

B

	Background	FITC-S1P	FITC-S1P +TNFα
Mean	348	867	501
SEM	72	110	116
number	6	6	6

Shown are the mean fluorescence intensity data (arbitrary units; collected from wild-type VSMCs by FACS analysis) that was subsequently normalized and presented as S1P uptake values in Figure 6B. All groups were statistically different from each other ($P<0.05$); both FITC-S1P groups shared the same background control (unlabeled S1P).

C

	Background	FITC-S1P	FITC-S1P + TNFα (24h)	FITC-S1P + TNFα (48h)	FITC-S1P + TNFα (24h) / Wash (24h)	FITC-S1P + TNFα (12h) / Wash (36h)
Mean	73	1265	541*	487*	934	1186
SEM	24	167	75	84	95	130
number	4	4	10	6	6	6

Shown are the mean fluorescence intensity data (arbitrary units; collected from wild-type VSMCs by FACS analysis) that was subsequently normalized and presented as S1P uptake values in Figure 6D. All groups were statistically above the background level. * denotes $P<0.05$ from the FITC-S1P group.

SUPPLEMENTAL TABLE 2*:* ***Mouse characteristics and cardiac function in sham and heart failure mice***

	sham saline	HF saline	sham etanercept	HF etanercept	n
Body weight (g)	27.4±0.8	27.8±0.6	27.9±0.6	27.8±0.6	12
Heart weight (mg)	162±11	206±14 *	166±7	180±9	12
Heart/Body Ratio	5.33±0.26	7.81±36 *	5.59±0.33	6.30±0.31	12
Lung weight (mg)	149±9	230±24 *	159±7	170±7	12
Liver weight (g)	1.23±0.03	1.40±0.04 *	1.31±0.04	1.27±0.04	12
Heart rate (min-1)	334±11	308±17	313±23	351±16	8
LVEF (%)	63±3	35±2 *	64±3	55±4	8
LVESP (mmHg)	122±2	107±2 *	123±4	105±6 *	8
LVEDP (mmHg)	1.3±0.2	7.0±2.2 *	2.384±0.805	6.2±1.4*	8
Stroke volume (μl)	178±7	107±15 *	189±26	142±27	8
MAP (mmHg)	86±2	72±5 *	88±2	85±2	8
CO (ml/min)	5.9±0.2	3.5±0.5 *	6.3±0.9	4.3±0.7	8
TPR (mmHg/ml)	15±1	27±4 *	16±2	24±5	8

Data are mean±SEM. ****P*<0.05 unpaired, multiple comparisons to sham saline control.

Acronyms: %LV – % of left ventricular wall; LVEF – Left ventricular ejection fraction; LVESP – Left ventricular end systolic pressure; LVECP – Left ventricular end diastolic pressure; MAP – mean arterial pressure; CO - cardiac output; TPR – total peripheral resistance.

With the exceptions of body weight and heart rate, heart failure (HF) significantly altered all mouse characteristic and cardiac function parameters assessed. Compared to the saline-treated control, etanercept had no effect on any parameter assessed. However, etanercept ameliorated the heart failure-induced changes to all parameters except LVEDP and LVESP.

SUPPLEMENTAL TABLE 3*:* ***RT-PCR Primers***

Target	Primer Sequences	Amplicon Size	Anneal Temp
GAPDH	Forward: 5'-TTCACCACCATGGAGAAGG-3' Reverse: 5'-CTCGTGGTTCACACCCATC-3'	111bp	55°C
CFTR (1)	Forward: 5'-TCGTGATCACATCAGAAATTATTGATAAT-3' Reverse: 5'-CCACCTCTCTCAAGTTTTCAATCAT-3'	99bp	55°C
CFTR (2)	Forward: 5'-AAAGAAAATATCATCTTTGGTGT-3' Reverse: 5'-TATACTGCTCTTGCTAAAGAAAT-3'	182bp	46°C
CFTR (3)	Forward: 5'-TCGTGATCACATCAGAAATTATTGATAAT-3' Reverse: 5'-CCACCTCTCTCAAGTTTTCAATCAT-3	99bp	50°C
Sphk1	Forward: 5'-ACCCCTGTGTAGCCTCCCT-3' Reverse: 5'-TGCAGTTGATGAGCAGGTCT-3'	107bp	55°C
SPP1	Forward: 5'-ATTTGCTTTTGCCTGTTTGG-3' Reverse: 5'-TGGCTATAGGATCTGGGTGC-3'	106bp	55°C
$S1P_2R$	Forward: 5'- AAAACCAACCACTGGCTGTC -3' Reverse: 5'- CTCTGAGTATAAGCCGCCCA -3'	104bp	55°C
β-Actin	Forward: 5'- GGCACCACACCTTCTACAATG Reverse: 5'-TGGATGGCTACGTACATGGCTG	620bp	55°C

SUPPLEMENTAL FIGURE 1

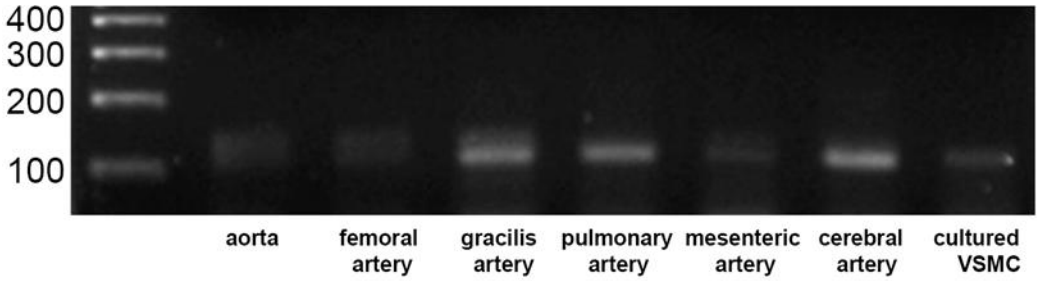

CFTR mRNA expression throughout the arterial vascular tree

RT-PCR experiments demonstrate CFTR mRNA expression in various sections of the arterial vascular tree, including aorta, cerebral, femoral, gracilis, pulmonary and mesenteric arteries. CFTR mRNA is also expressed in cultured vascular smooth muscle cells isolated from mesenteric arteries.

SUPPLEMENTAL FIGURE 2

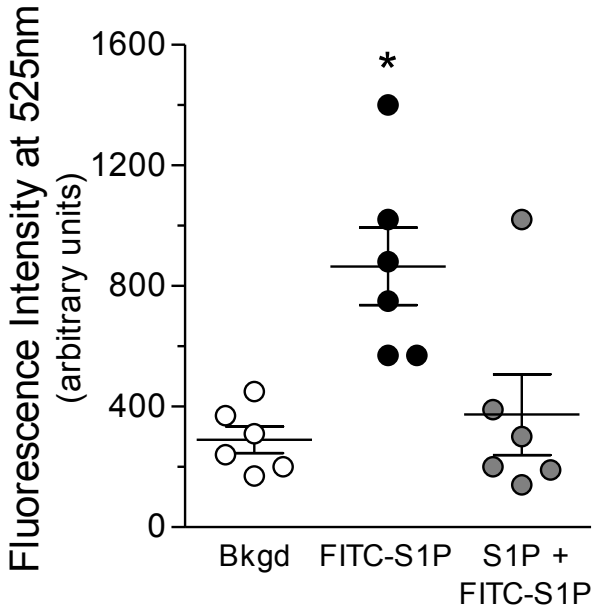

Unlabeled S1P co-incubation inhibits FITC-S1P uptake in cultured vascular smooth muscle cells

Utilizing a standard FACS analysis technique, a shift in the median fluorescence intensity at 525nm is observed for cultured vascular smooth muscle cells incubated with 1μmol/L FITC-S1P for 30 minutes (compared to background; Bkgd). When co-incubated with 1μmol/L unlabeled S1P, the uptake of FITC-S1P was abolished. * denotes $P<0.05$ for multiple, unpaired comparisons; n=6 for all groups.

SUPPLEMENTAL FIGURE 3

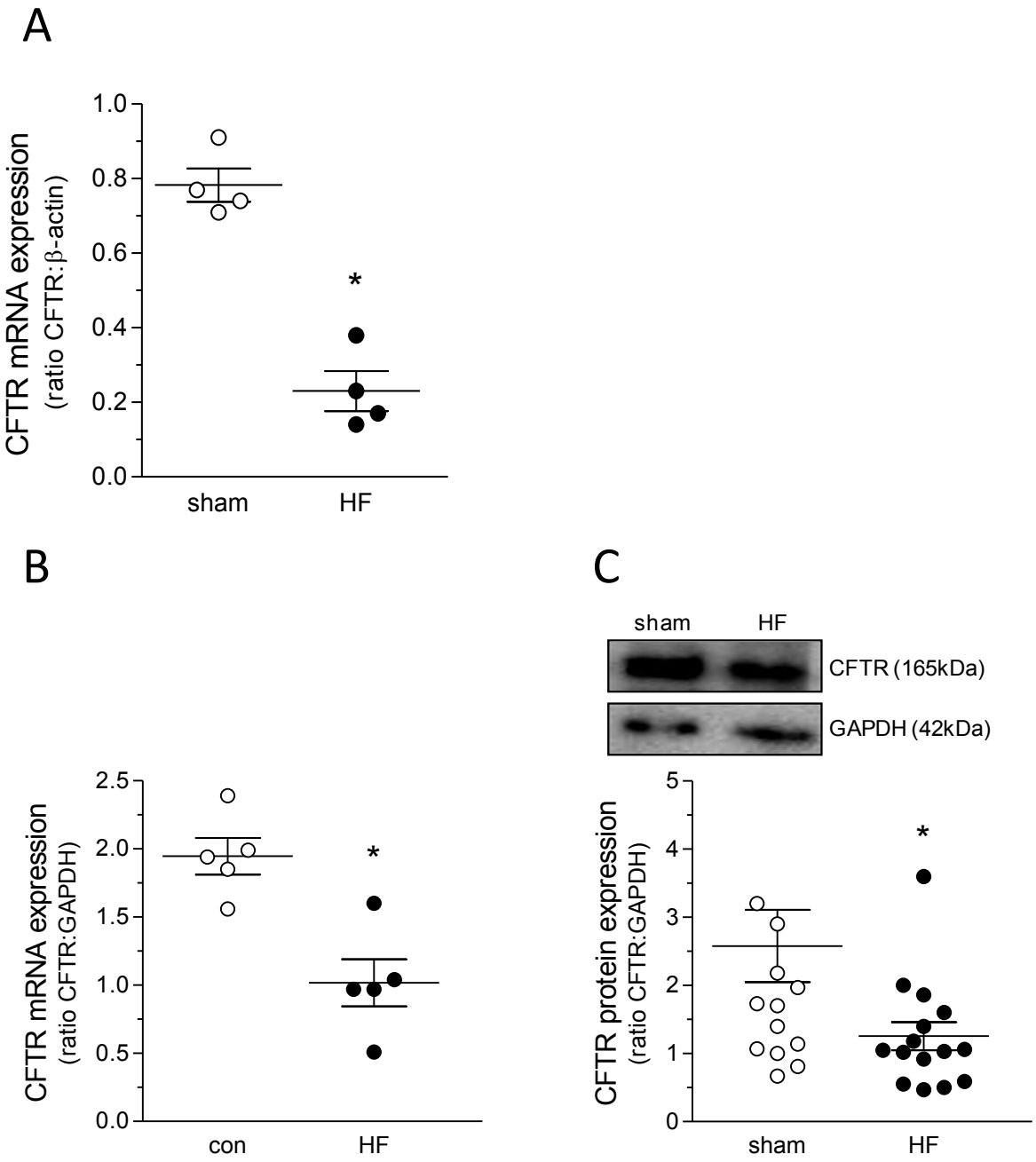

Heart failure down-regulates CFTR mRNA and protein expression in mouse resistance arteries

Heart failure (HF; 4-6 weeks post-myocardial infarction) was associated with a down-regulation of **(A)** posterior cerebral artery CFTR mRNA expression (n=4), **(B)** mesenteric artery CFTR mRNA expression (n=5) and **(C)** mesenteric artery CFTR protein expression (n=16). * denotes $P<0.05$ for single, unpaired comparisons.

SUPPLEMENTAL FIGURE 4

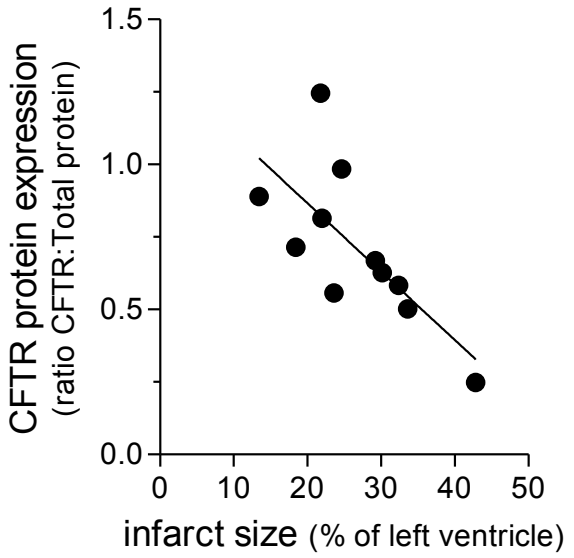

CFTR expression is negatively correlates with infarct size in mesenteric arteries

In mouse mesenteric arteries, CFTR expression negatively correlated with the extent of the myocardial infarction (n=11).

SUPPLEMENTAL FIGURE 5

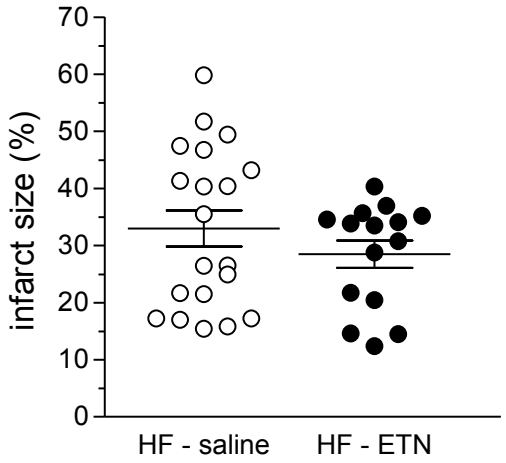

Etanercept treatment does not reduce infarct size following left anterior descending artery ligation

Ligation of the left anterior descending artery results in a reproducible infarction (~30%) of the left ventricle. Etanercept treatment, which was initiated immediately after setting the infarct, did not impact the degree of myocardial infarction. Data are analyzed with an unpaired t-test; n=20 for heart failure mice treated with saline vehicle (HF-saline) and n=15 for heart failure mice treated with etanercept (HF-ETN).

SUPPLEMENTAL FIGURE 6

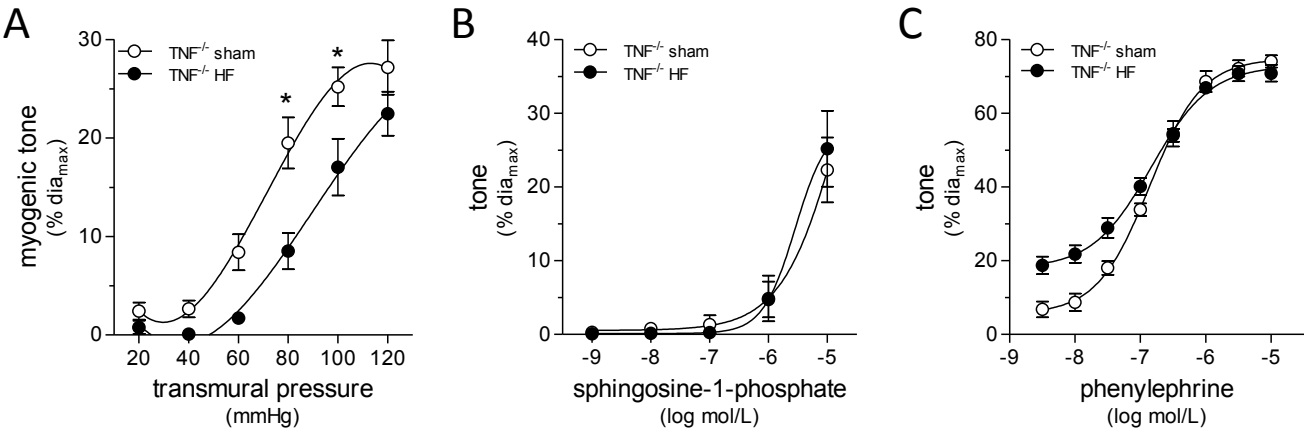

Heart failure does not enhance myogenic tone or S1P responsiveness in mesenteric arteries isolated from TNFα knockout mice

In mesenteric arteries isolated from $TNF^{-/-}$ mice, HF failed to enhance myogenic tone **(A).** In fact, myogenic tone was significantly decreased at 80mmHg and 100mmHg, compared to the sham control. Heart failure did not affect S1P-stimulated vasoconstriction **(B)** or responses to phenylephrine **(C)**. * denotes $P<0.05$ following a Wilcoxon test with computation of exact *p*-values as a post-test following two-way repeated measures ANOVA analysis. $TNF^{-/-}$ sham dia_{max}=209±9μm, n=7; $TNF^{-/-}$ HF dia_{max}=187±6μm, n=8 (P=N.S.).

SUPPLEMENTAL FIGURE 7

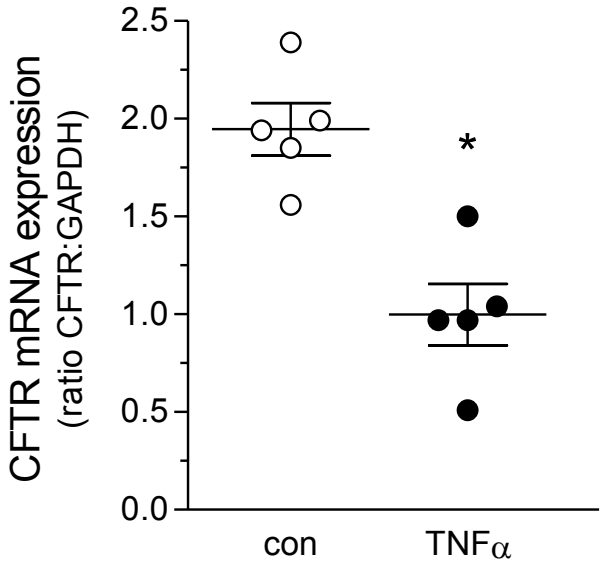

Heart failure and TNFα down-regulate vascular CFTR mRNA expression.

TNFα exposure (10ng/ml; 24hrs) stimulated the down-regulation of CFTR mRNA expression in vascular smooth muscle cells isolated from mouse mesenteric arteries (n=5). * denotes $P<0.05$ for single, unpaired comparisons.

SUPPLEMENTAL FIGURE 8

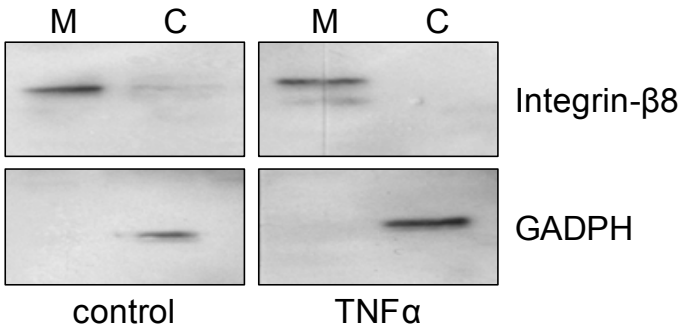

Verification of successful cellular fractionation

Western blots demonstrate the successful separation of plasma membrane and intracellular fractions. In fractions prepared from both control and TNFα-treated (10ng/ml, 24 h) cells, the plasma membrane marker integrin-β8 (72kDa) is only detected in the membrane (M) fraction, while the cytosolic marker GAPDH (39kDa) is only detected in the cytosolic fraction (C).

SUPPLEMENTAL REFERENCES

1. Sharma M, Benharouga M, Hu W, Lukacs GL. Conformational and temperature-sensitive stability defects of the delta F508 cystic fibrosis transmembrane conductance regulator in post-endoplasmic reticulum compartments. *J Biol Chem*. 2001; 276:8942-8950.

2. Bordier C. Phase separation of integral membrane proteins in Triton X-114 solution. *J Biol Chem*. 1981; 256:1604-1607.

3. Wang Y, Loo TW, Bartlett MC, Clarke DM. Additive effect of multiple pharmacological chaperones on maturation of CFTR processing mutants. *Biochem J*. 2007; 406:257-263.

4. Thibodeau PH, Richardson JM, III, Wang W, Millen L, Watson J, Mendoza JL, Du K, Fischman S, Senderowitz H, Lukacs GL, Kirk K, Thomas PJ. The cystic fibrosis-causing mutation deltaF508 affects multiple steps in cystic fibrosis transmembrane conductance regulator biogenesis. *J Biol Chem*. 2010; 285:35825-35835.

5. Hochman JS, Choo H. Limitation of myocardial infarct expansion by reperfusion independent of myocardial salvage. *Circulation*. 1987; 75:299-306.

6. Hoefer J, Azam MA, Kroetsch JT, Poi HL, Momen MA, Voigtlaender-Bolz J, Scherer EQ, Meissner A, Bolz SS, Husain M. Sphingosine-1-Phosphate-Dependent Activation of p38 MAPK Maintains Elevated Peripheral Resistance in Heart Failure Through Increased Myogenic Vasoconstriction. *Circ Res*. 2010; 107:923-933.